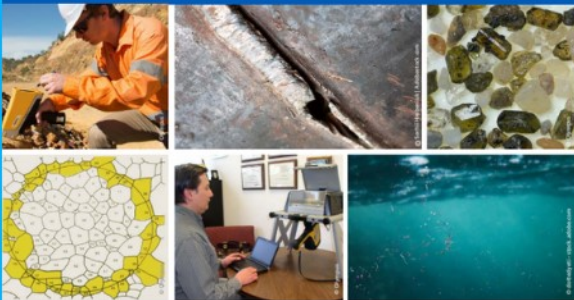




2nd Advanced Optical Metrology Compendium

Advanced Optical Metrology

Geoscience | Corrosion | Particles | Additive Manufacturing: Metallurgy, Cut Analysis & Porosity



EVIDENT
OLYMPUS

WILEY

The latest eBook from **Advanced Optical Metrology**.
Download for free.

This compendium includes a collection of optical metrology papers, a repository of teaching materials, and instructions on how to publish scientific achievements.

With the aim of improving communication between fundamental research and industrial applications in the field of optical metrology we have collected and organized existing information and made it more accessible and useful for researchers and practitioners.

EVIDENT
OLYMPUS

WILEY

Smart Skin-Adhesive Patches: From Design to Biomedical Applications

Siu Hong Dexter Wong, G. Roshan Deen, Jeffrey S. Bates, Chiranjit Maiti, Ching Ying Katherine Lam, Abhishek Pachauri, Renad AlAnsari, Petr Bělský, Jinhwan Yoon,* and Jagan Mohan Dodda*

With the advancement of medical and digital technologies, smart skin adhesive patches have emerged as a key player for complex medical purposes. In particular, skin adhesive patches with integrated electronics have created an excellent platform for monitoring health conditions and intelligent medication. However, the efficient design of the adhesive patches is still challenging as it requires a strong combination of network structure, adhesion, physical properties, and biocompatibility. To design an assimilated device, one must have a deep knowledge of various skin adhesive patches. This article provides a comprehensive review of the recent advances in skin-adhesive patches, including hydrogel-based adhesive patches, transdermal patches, and electronic skin (E-skin) patches, for various biomedical applications such as wound healing, drug delivery, biosensing, and health monitoring. Furthermore, the key challenges, implementable strategies, and future designs that can potentially provide researchers in designing innovative multipurpose smart skin patches are discussed. These advanced approaches are promising for managing the health and fitness of patients who require regular medical care.

1. Introduction

The collective progress in medical, electronics, and digital technologies has entailed exponential growth in developing biocompatible health monitoring patches such as skin-adhesive patches, E-skin patches, wearable sensors, blood pressure monitors, optoelectronic devices, fitness trackers, and transdermal patches. These patches not only help monitor the


health situation of patients but also offer professional advice or/and local treatment to improve their health conditions.^[1] The functionalities can be realized by smart patches that comprise multiple integrated components, including drug reservoirs, drug carriers, a transfer device, and sensors.^[2] In particular, E-skin devices integrated with miniaturized biosensors can detect the physiological and biomechanical status of the body via communicating with skin tissues as an effective in situ diagnostic tool for further implementation in clinical practice at personal patient levels.^[3] Furthermore, wearable transdermal drug delivery system (TDDS) has been prevalent for noninvasive and stimuli-responsive drug release via permeating skin structure to the bloodstream, enabling treatment on purpose (auto-medication).^[4] Numerous recent studies reported various types of skin-patchable devices for

different biomedical applications, including drug delivery,^[2,5] wound healing,^[6] treatment of myocardial infarction,^[7] and tissue engineering.^[8] To this end, advanced technologies from different fields, including selection of correct materials (e.g., biopolymers and nanomaterials),^[9] adopting suitable fabrication methods (e.g., soft lithography and 3D printing)^[10] and designing specific biochemical reactions have been to fabricate functional skin patches for transdermal theragnostics.

S. H. D. Wong, C. Y. K. Lam
Department of Biomedical Engineering
The Hong Kong Polytechnic University
Kowloon, Hong Kong 999077, China

G. R. Deen, R. AlAnsari
Materials for Medicine Research Group
School of Medicine
The Royal College of Surgeons in Ireland (RCSI)
Medical University of Bahrain
Busaiteen 228, Bahrain 15503, Kingdom of Bahrain

J. S. Bates, A. Pachauri
Materials Science and Engineering
University of Utah
122 S. Central Campus Drive, Room 304, Salt Lake City, UT 84112, USA

 The ORCID identification number(s) for the author(s) of this article can be found under <https://doi.org/10.1002/adfm.202213560>.

C. Maiti, J. Yoon
Graduate Department of Chemical Materials
Institute for Plastic Information and Energy Materials
Sustainable Utilization of Photovoltaic Energy Research Center
Pusan National University
Busan 46241, Republic of Korea
E-mail: jinhwan@pusan.ac.kr

P. Bělský, J. M. Dodda
New Technologies—Research Centre (NTC)
University of West Bohemia
Univerzitní 8, Pilsen 30100, Czech Republic
E-mail: jagan@ntc.zcu.cz

DOI: 10.1002/adfm.202213560

A clinically approved smart skin patch should meet several criteria, such as good biocompatibility and mechanical property, firm grip on the skin, easy operation, painlessness, and minimal side effects. Recently developed wearable E-skin patches are composed of thin, flexible, and lightweight films embedded with sensing electronics for monitoring health conditions by continuously probing bio-analytes from biofluids, including sweat, tears, and salivary,^[11] and also tracking physiological parameters such as body temperature, heart rate, blood pressure, blood oxygen level, respiration rate.^[12] Commercially available hardware devices may be able to achieve these functions, but several key challenges are yet to be addressed, including smooth contact and good adhesion between the skin and the rigid electronics, mechanical stability of the patches against rapid stress–strain loading, long-term durability, compatibility between the substrate layer and the electronics, low limit of detection, and overall system calibration for analyzing signals and biofluids. Thus, an in-depth understanding of existing/developed smart wearable patches is crucial for designing next-generation multifunctional patches.

This review highlights the recent advances in constructing biomedical patches, including skin adhesive hydrogel patches, transdermal patches, and E-skin patches. Furthermore, we summarize different approaches to prepare transdermal patches, the mechanism underlying the adhesion mechanisms between the skin and the hydrogel patch, and the principle of E-skin biosensory that together provide useful references for developing self-monitoring and auto-medication skin patches. Although specific types of wearable skin patches have been discussed by several reviews,^[13] there is a lack of comprehensive review that covers the design, skin adhesion, biocompatibility and commercial feasibility. We break our review into several sessions: 1) summarizing types of materials and techniques for the fabrications, 2) reviewing representative examples of transdermal patches and E-skin patches, and 3) discussing the key challenges and expressing our perspectives about implementable strategies for designing innovative multipurpose smart skin patches for patients who require regular healthcare monitoring and medication.

2. Hydrogel-Based Skin Adhesive Patches

The recent development of hydrogel-based skin patches with unique functionalities for biomedical applications covers diverse research areas, including real-time health monitoring, controlled transdermal drug delivery, and wound care management, etc.^[14] To design biocompatible skin-adhesive patches, hydrogels are the ideal component of the patch owing to their biomimetic structure and tunable physiochemical properties.^[14e,15] By definition, a hydrogel consists of a three-dimensional crosslinked polymer chain network that is highly hydrophilic and can entrap a significant amount of water molecules within the network, leading to its water content of over 70%.^[16] This highly water-absorbable property is hardly achieved by conventional polymer fraction that imposes challenges for maintaining suitable attachment to skin tissues via chemical/physical interactions.^[17] To overcome this limitation, researchers often incorporate various chemical groups

into the polymer backbones to improve their hydrophilicity and adhesiveness to form skin-adhesive hydrogels.^[18] In this section, we introduce hydrogel adhesives that show an inherent capability to attach to skin surfaces without using external glues.

2.1. Adhesion Mechanism for Hydrogel Skin Patch

Recently, researchers have developed diverse natural and synthetic polymer-based hydrogel skin adhesives with a range of bonding chemistry (covalent and noncovalent).^[14d,15b,18a,19] TDDS is one of the major applications of skin adhesive hydrogel patches that load therapeutics into the hydrogel matrix while adhering to skin surfaces for the effective delivery of drug molecules in a noninvasive and improved patient compliance way. For this purpose, strong skin adhesion and long-term stability, and biocompatibility are essential.

Inspired by the adhesion mechanism found in marine organisms (e.g., mussels), researchers designed phenolic compound-based adhesive hydrogels, especially possessing catechol moiety that can extensively form strong covalent and noncovalent bonds with the organic surface in the presence of water (wet-binding).^[20] Thus, the adhesion mechanisms can be attributed to these versatile bonding chemistries, typically categorized as physical bondings, including hydrogen bonding, metal complexation, π – π and cation– π interactions via the aromatic groups; chemical bondings that the oxidized catechol (quinone) bonds with imines, amine or thiol groups or other catechols.^[20c,21] Recently, Jung et al. synthesized an ultra-adhesive hydrogel consisting of photocrosslinked of acrylamide (AM) in the presence of polydopamine (PDA) and homogeneously mixed extra-large pore (20–30 nm) mesoporous silica nanoparticles (XL-MSNs). This hydrogel also showed superior mechanical properties and strong tissue adhesiveness (**Figure 1a**).^[22] The PDA component permitted the inherent adhesive property via the formation of irreversible covalent and reversible noncovalent interactions with the skin surface. The XL-MSNs allowed efficient encapsulation of the drug for controlled release. Moreover, the hydrogel showed a 4.9-fold increase in adhesive property with adhesion energy of 151 J m^{-2} to porcine skin tissue after incorporating appropriate amounts of XL-MSNs, which contributed to the synergistic enhancement of cohesiveness, probably because of the physical crosslinking between XL-MSNs with the polymer chains and skin tissues. This study demonstrates the importance of fabricating nanocomposite polymers as an effective biopatch, hydrogel glue and TDD system.

Similarly, Han et al. also prepared an adhesive and conductive hydrogel composed of PDA-decorated carbon nanotubes (CNTs) incorporated in AM and acrylic acid-based hydrogel using a binary-solvent system composed of water and glycerol for the synthesis.^[23] The PDA-decorated CNTs provided good conductivity and promoted the overall mechanical properties of the hydrogel. The combination of PDA and viscous glycerol on catechol groups empowered its adhesive strength of $\approx 60 \text{ kPa}$ at room temperature. Furthermore, the hydrogel allowed operation over a wide temperature range (-20 to $60 \text{ }^\circ\text{C}$), making it a promising material as bio-adhesive bioelectronics to detect

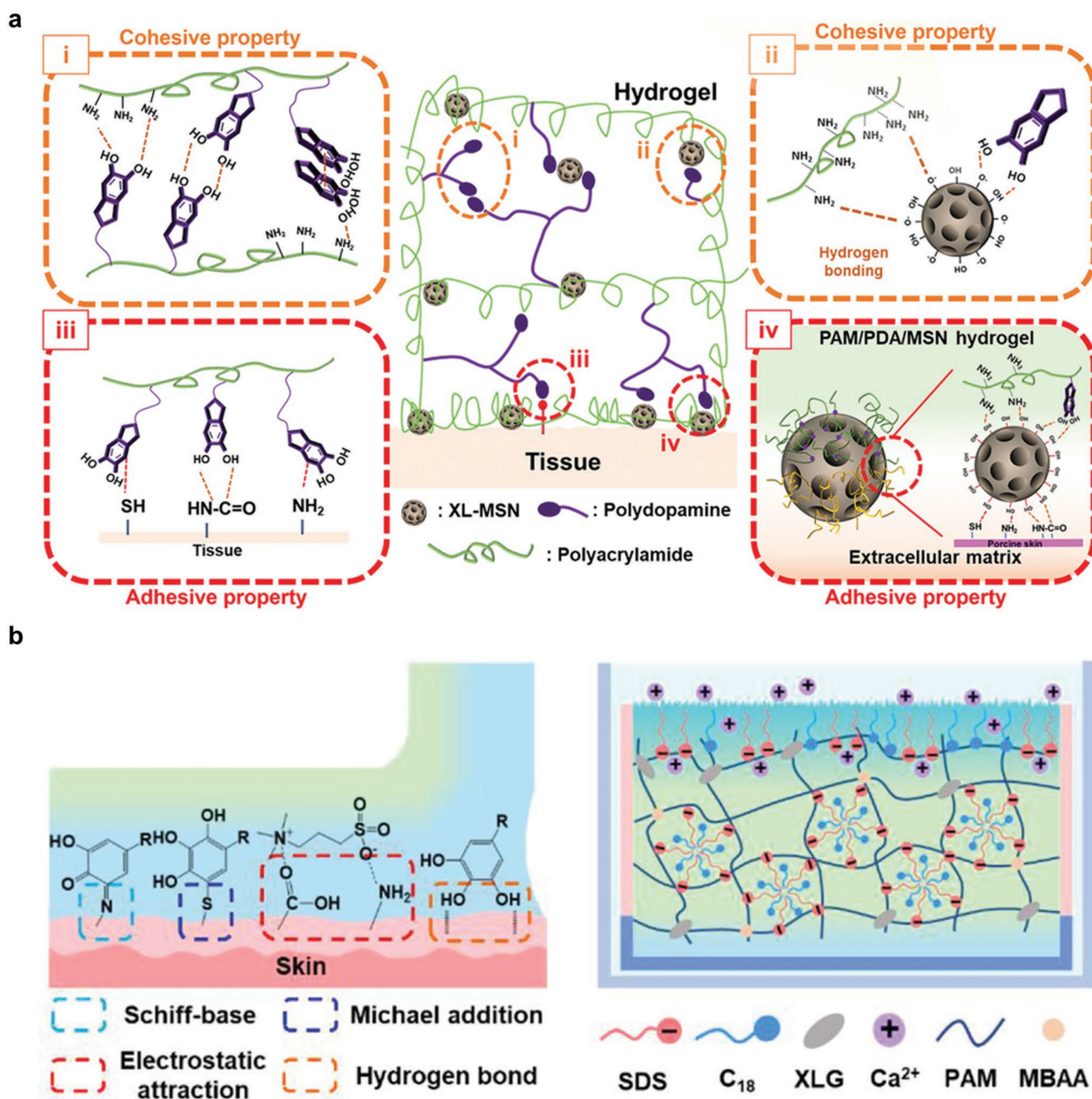


Figure 1. a) Schematic illustration of a polydopamine (PDA) based skin adhesive hydrogel patch with different types of representative molecular interactions between the hydrogel and skin tissues associated with synergistic enhancement of i,ii) cohesive and iii,iv) adhesive properties. Reproduced with permission.^[22] Copyright 2020, Wiley-VCH. b) Schematic illustration of the (left) adhesion mechanisms with the skin surfaces and (right) hydrophobic bilayer hydrogel matrix formation of adhesive and hydrophobic bilayer hydrogel. Reproduced with permission.^[24] Copyright 2022, Wiley-VCH.

biological signals in cold or hot environments and a dressing material to protect skin from frostbites or burns. This work provides a novel insight into the fabrication of antifreezing and antiheating hydrogels with multifunctionality.

Hydrogel-based epidermal electrodes have drawn widespread attention in health monitoring and human electronic interfaces by offering excellent biocompatibility, tissue-mimetic mechanical property, and stable in situ electrophysiological recording performance. For instance, Liu et al. developed an

ionic hydrogel using polyvinyl alcohol (PVA) and branched polyethyleneimine (b-PEI) composited with calcium chloride (CaCl_2) to formulate skin-adhesive epidermal electrodes for real-time health monitoring.^[25] This hydrogel exhibited body temperature-enhanced superior stretchability of 1291% with skin-matched Young's modulus ≈ 10 kPa with an adhesive energy of ≈ 60 J m^{-2} , a stable ionic conductivity of 3.09 S m^{-1} , and outstanding antibacterial ability. The hydrogel crosslinking strategy was achieved by which hydroxyl groups ($-\text{OH}$) of PVA

formed hydrogen bonds (H-bond) with amino groups ($-\text{NH}_2$) of b-PEI and CaCl_2 helped construct the coordination between $-\text{OH}/-\text{NH}_2$ and Ca^{2+} within the polymer chains to well support adhesion to the skin. In particular, this hydrogel was temperature-sensitive and the body temperature (37°C), further promoted gapless adhesion with the skin because of the sol-gel transition that decreased the viscosity. This ionic hydrogel-based epidermal electrode exhibited a high signal-to-noise ratio and a low detection limit (LOD) at the μV -scale for measuring the electrophysiological signals. In addition, the positively charged b-PEI in the hydrogel showed high antibacterial activity against *Escherichia coli* and *Staphylococcus aureus*, preventing bacterial infections in the human skin. Thus, this study demonstrated the unique merit of ionic hydrogels as multifunctional and soft electrodes in real-time electrophysiological recording to study the electrical properties of biological cells and tissues in nervous systems.

Human emotion recognition is traditionally characterized by electroencephalogram (EEG), which relies on rigid electrodes and lacks anti-interference and portability. To overcome these barriers, Yang et al. synthesized a hydrogel-based advanced biosensor with a hydrophobic bilayer for high-fidelity measurements and classification of human emotions.^[24] The adhesive hydrogel was primarily composed of covalently crosslinked polyacrylamide and poly[2-(methacryloyloxy)ethyl]dimethyl-(3-sulfopropyl) ammonium hydroxide (Figure 1b). The additional micellar aggregation composed of hydrophobic chains and surfactants further enhanced the robust coupling between the layers of hydrogel functional matrices. The incorporation of Laponite XLG and catechol functionality presented in Tannic acid, Al^{3+} ion, and glycerin improved the adhesion performance remarkably, with up to an adhesion strength of $\approx 59.7\text{ N m}^{-1}$. This specially designed hydrogel performed well in collecting and classifying electrophysiological signals for EEG-based motion recognition under vibration, sweating and stable monitoring conditions. These findings reveal critical insights into portable and hydrogel-based headbands for the diagnosis of neurological diseases with high measurement performances.

To better understand the designing principle of skin-adhesive patches for optimal adhesive performance, one should also consider the underlying adhesive contact mechanics of soft materials. The interaction of adhesive tractions between different types of skin and adhesive patches should be considered. In this case, classical contact mechanics or the Signorini dichotomy cannot theoretically explain the adhesive tractions between two interacting systems where interacting solid bodies should be non-tensile. As the skin-adhesive patch system should be considered a deformable contacting system, the approximation introduced in Signorini dichotomy with an analysis of the deformation introduced by Johnson et al. provides a convenient and reliable solution and is known as Johnson, Kendall, and Roberts theory or JKR solution.^[26] Macroscopic roughness in the skin surface is also an important parameter to be considered. Many authors developed models to quantitatively characterize the effect of surface roughness on adhesion.^[27] For nanoscale measurements of adhesion tractions, the theory of peeling provided by Kendall can be classically explained in the most famous case of gecko feet, whose feet adhesion can sustain several times its weight, while also being able to completely detach its foot in

15 ms.^[28] This phenomenon has also been implemented theoretically and verified experimentally by many researchers.^[29]

2.2. Hydrogel Skin Patches of Tunable Adhesion

When designing skin-adhesive hydrogel patches, one should notice that the level of adhesion strength plays an important role in precise biomedical application on skin with different properties. For instance, a patch with too strong adhesiveness is unsuitable for premature or fragile skin surfaces as it may cause pain, skin damage, inflammation, or irritation during detachment.^[30] Therefore, developing skin-friendly hydrogel adhesives with tunable adhesion strength is highly desirable for implementing noninvasive transdermal diagnosis and therapy.

Recently, Lee et al. reported a polyampholyte terpolymer (PAT)-based hydrogel with tunable adhesion properties by modifying the hydrogel network structure at the molecular level without any surface modification (Figure 2a).^[31] The PAT hydrogel was synthesized by mixing two oppositely charged monomers, 3-(methacryloylamino)propyl-trimethylammonium chloride (cationic monomer) and sodium *p*-styrenesulfonate (anionic monomer), with the optimum amount of *N,N*-dimethylacrylamide (a neutral monomer) to maintain an overall neutral charge. The incorporation of the neutral monomers in the hydrogel network produced more structural defects in the ion-pair associations as the regulator of adhesion strength.

Designing reversible and smart stimuli-responsive hydrogel has been a sound footing strategy for triggering adhesion and detachment.^[33] For example, Jiang et al. demonstrated a hydrogel consisting of poly(gallic acid) complexed with gelatin methacrylate (GelMA), which was further polymerized with poly(ethylene glycol) diacrylate (Figure 2b).^[33c] This hydrogel patch showed body temperature-induced adhesion to the skin and painless detachment achieved by the cooling effect. In a detailed explanation, the hydrogel was softened by the body temperature of the skin due to the decomplexation of GelMA polymer chains, resulting in strong adhesion. On the other hand, the authors applied an ice bag for the cool effect that enhanced re-entanglement GelMA chains via intermolecular H-bonds and drastically reduced its adhesion property. The hydrogel patch in porcine skin maintained average adhesion energy of $\approx 8.1\text{ J m}^{-2}$ at body temperature, whereas it lost adhesion properties upon ice-cooling. Moreover, their findings justified that this hydrogel was friendly for infant skin and acted as epidermal bioelectronics for long-term health monitoring and wound dressing for diabetic patients.

Zhao et al. also developed a conductive and detachable bioadhesive hydrogel based on graphene oxide (GO) nanocomposites.^[33b] The authors integrated GO into a PVA hydrogel which was further crosslinked with poly(acrylic acid) grafted with *N*-hydroxysuccinimide (NHS) ester. Furthermore, the reduction of GO (rGO) improved the electrical conductivity of the hydrogel without affecting its mechanical property. The hydrogel formed strong adhesion on diverse wet tissue surfaces within 5 s with only a gentle press ($\approx 1\text{ kPa}$). The PVA chain presented numerous carboxylic acid groups that permitted rapid absorption of the interfacial water and formed physical crosslinks, including H-bond and electrostatic interactions with

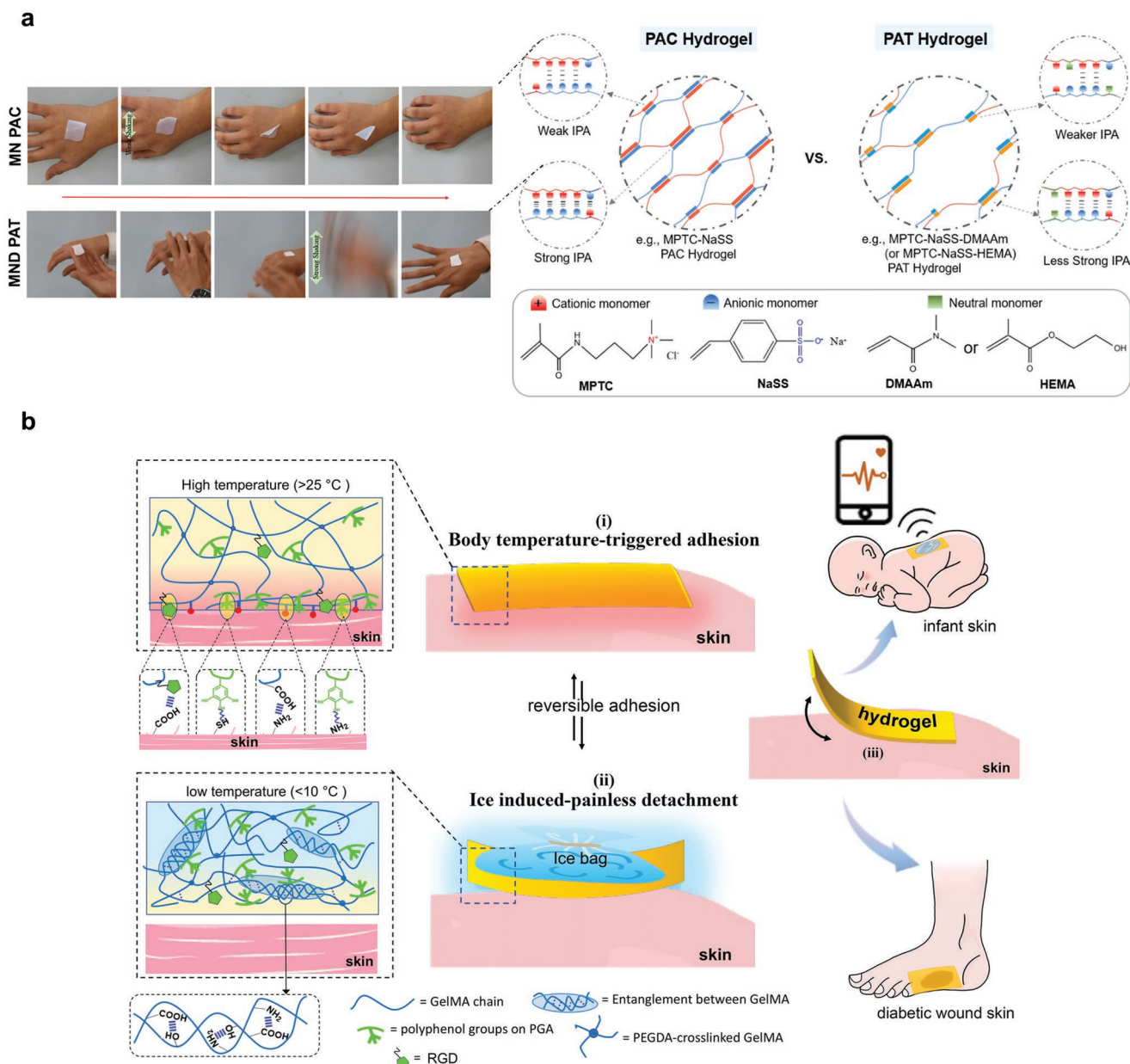


Figure 2. a) Adhesion performance of the MPTC-NaSS polyampholytic copolymer (PAC) hydrogel (top) and the MPTC-NaSS-DMAAm polyampholytic terpolymer (PAT) hydrogel (bottom) examined via respective shaking of hand weakly and strongly. Reproduced with permission.^[31] Copyright 2021, American Chemical Society. b) Schematic illustrations of the body temperature-triggered skin-friendly adhesion and ice-cooling-induced painless detachment of the PGA-GelMA hydrogel. Reproduced with permission.^[32] Copyright 2022, American Chemical Society.

the skin tissue. Besides, the NHS ester groups formed additional covalent crosslinks with primary amine groups of the tissue surface to reinforce the adhesion. In contrast, the e-bioadhesive could be detached from the skin in response to aqueous reduced glutathione or sodium bicarbonate. In short, these studies provide rationale guidance toward stimuli-response hydrogel patches for enhanced skin adhesion and friendly detachment to minimize undesirable effects post-treatment/diagnosis.

Recently, Bao et al. reported the development of smart hydrogel bandages of tunable adhesion, which is achieved by

the volume phase transition of the hydrogel network.^[34] The hydrogels of double network structure consisting of thermo-responsive poly(*N*-isopropyl acrylamide-*ran*-acryl amide) (p(NIPAM-*ran*-AM) copolymer and conductive poly(3,4-ethylenedioxythiophene):polystyrene sulfonate (PEDOT:PSS) were prepared as an adhesive electrode for the bandages. While the prepared hydrogel electrodes exhibited strong adhesion at normal skin temperature, the adhesion force dramatically reversibly decreased over 40 °C owing to the phase transition of the p(NIAPM-*ran*-AM). Below the lower critical solution temperature (LCST), the p(NIAPM-*ran*-AM) shows a preferable

interaction with skin to provide a strong interfacial adhesion, which is no longer effective over LCST due to the aggregation of the backbones.

3. Transdermal Patches for Biomedical Applications

TDDS has emerged as an alternative to oral drug administration as it can overcome patient compliance and the effects on the gastrointestinal (GI) tract.^[14e,35] In transdermal delivery, the solute (therapeutic agent) diffuses through the various layers of the skin and into the systemic circulation. The major advantages of transdermal drug delivery are listed as follows: i) the first-pass metabolism and GI tract effects are avoided, ii) side effects that are associated with systemic toxicity are reduced, iii) improved patient compliance, iv) direct skin infection targeting, v) painless administration, and vi) ease of use.

In 1979, the first transdermal patch containing scopolamine for the prevention of motion sickness was approved by the US Food and Drug Administration (FDA). Later, transdermal patches for analgesic activity, contraception, hormone replacement therapy, and prevention of angina pectoris were approved and marketed. Since the 1980s, the market for transdermal patches has increased tremendously to a value of 31.5 billion US dollars.^[36] A few important transdermal patches that are currently on the market are summarized in **Table 1**. Patches containing single therapeutic agents such as clonidine, lidocaine, fentanyl, nitro-glycerine, oxybutynin and testosterone, and patches containing a combination of drugs are available in the market. Depending on the nature of the drugs, the patches can often extend the delivery duration over 1 week.

Hydrogels are the ideal personalized medicine as a transdermal patch for biomedical applications. The polymeric network of hydrogels imparts properties of solid- and liquid-like characteristics for orchestrating various device shapes and dissolving biomolecules for the controlled release of drugs, respectively.^[38] The soft and moisturized nature of hydrogels enables smooth contact with different skin textures.^[39] Together with the tunable porous network of hydrogels that entrap drugs and sustain their release to the skin,^[40] these physicochemical properties of hydrogels are highly favorable to tailor-make a

functional and moisture interface between the transdermal patch and human skin for therapy. In this section, we discuss the design and mechanism for different types of skin adhesive patches to maximize their transdermal delivery. We also summarize examples of recent advances in hydrogel-based skin patches for biomedical applications such as drug delivery and wound healing.

3.1. Enhancing Skin Permeation: Passive and Active Methods

Despite the numerous attractive advantages, transdermal delivery also has its own limitations. The major obstacle is the hindered or slow diffusion of drugs across the epidermis of the skin (stratum corneum).^[41] As a result, drug molecules that meet specific physicochemical criteria such as low-molar mass (<500 Da), low melting point (<150 °C), acceptable lipid and water solubility, and high potency (total daily dose < 10 mg) can only be used in transdermal drug delivery. Over the last two decades, several approaches have been introduced to overcome skin barrier issues for transdermal drug delivery of a variety of drugs. Generally, the main approaches can be categorized into passive and active methods.

For the passive method, drugs are loaded into the patch as forms of ointments, gels, or creams and their release relies on only diffusion. Since good epidermal permeability and high diffusion rate are required for efficient drug delivery, liposomes, vesicles, penetration enhancers, and supersaturated systems are typically used to assist skin absorption of the drugs with a controlled dosage.^[11,12,42] Since the dimension of the patches is usually designed to be less than 40 cm² for cosmetic reasons and patient comfort, the total amount of drug loading and its release are limited by the small dimension. To deliver more drug through a smaller patch area, DOT Matrix transdermal drug delivery platform has been developed by Noven pharmaceuticals.^[43] In this technique, concentrated drug micro-cells are formed by drug-loaded polymer particles with a very large surface area, enabling highly efficient diffusion-based drug release from the skin patch of a small area.

Typical commercialized therapeutic molecules, including peptide- and protein-based drugs, have a large molar mass of more than 500 Da, which drugs can be degraded in the GI tract such

Table 1. Important commercially available transdermal patches.

Trade name ^[37]	Drug	Therapeutic use	Manufacturer	Diffusion rate
Alora	Estradiol	Postmenstrual syndrome	TheraTech/Proctor and Gamble	2.8 µg cm ⁻² per day
Androderm	Testosterone	Hypogonadism	TheraTech/Glaxo Smith Kline	0.33 mg cm ⁻² per day
Catapres-TTS	Clonidine	Hypertension	Alza/Boehinger Ingelheim	28.6 µg cm ⁻² per day
Climara	Estradiol	Postmenstrual syndrome	Ethical Holdings/Wyeth	3.8 µg cm ⁻² per day
Desponite	Nitroglycerine	Angina pectoris	Schwarz Pharma	15 µg cm ⁻² per hour
Fempatch	Estradiol	Postmenstrual syndrome	Parke-Davis	20 µg per day
Lidoderm	Lidocaine	Posttherpetic neuralgia	Janssens-Cilag	152 µg cm ⁻² per 12 h
Nicoderm	Nicotin	Smoking cessation	Alza/Glaxo Smith Kline	945 µg cm ⁻² per day
Nitrodisc	Nitroglycerine	Angina pectoris	Roberts Pharma	20 µg cm ⁻² per 1 h
Transderm Scop	Scopolamine	Motion sickness	Alza/Novartis	0.67 mg cm ⁻² per day

Table 2. Various active methods used for enhancing skin permeation.

Active method	Method
Electrical methods ^[44]	<p>Iontophoresis: Uses electric current (low level) directly on the skin or on the topically applied patch. The mechanism involves electro-repulsion, electro-osmosis, and electro-perturbation.</p> <p>Ultrasound: Uses ultrasound of a suitable frequency for a smaller area on the skin (phonophoresis or sonophoresis). The drug is mixed with a coupling agent for the transfer of an ultrasonic agent.</p> <p>Photomechanical waves: Involves the use of photochemical waves leading to the formation of transient channels through the stratum corneum.</p> <p>Electroporation: Uses short electrical pulses (100 to 1000 V cm⁻¹) to create aqueous pores in the lipid bilayers.</p> <p>Electro-osmosis: Uses voltage difference on a porous membrane to drive osmosis.</p>
Mechanical and structural methods ^[45]	<p>Micro needles (micro fabricated): Uses micro needles to form a physical pathway through the upper epidermis. Various approaches are: the poke with patch approach, coat and poke approach, microencapsulation approach, and hollow micro needles approach.</p> <p>Abrasion: The direct removal or modification of the upper layers of the skin is involved in this method. This leads to resurfacing the skin superficially.</p> <p>Stretching: Uses an expandable device to stretch the skin in unidirectional or multidirectional. This creates micro pathways for the efficient diffusion of drugs.</p> <p>Suction</p>
Velocity based methods ^[46]	<p>Needle-free injections: A pain-free method to administer drugs to the skin.</p> <p>Powder jet devices: In this method, solid particles of size 20–100 nm are fired through the stratum corneum into the lower layers of the skin. The process is usually carried out using a supersonic shock wave of helium gas.</p>
Other methods ^[47]	<p>Using liposomes that are encapsulated with drugs.</p> <p>Using modified liposomes (Transferosomes).</p> <p>Using a magnetic field to facilitate diffusion (Magnetophoresis).</p> <p>Using radio frequency waves to increase the diffusion of drugs.</p> <p>Using medicated tattoos containing active drugs.</p>

as by the action of digestive enzymes. Furthermore, these large molecules do not have high skin penetration ability with the aforementioned passive method aforementioned. To overcome this low efficiency, external energies are applied as a driving force to promote the skin permeation efficiency of the drugs, which is called active methods. We have enlisted several types of active methods for enhancing skin permeability in **Table 2**.

3.2. Design and Mechanism of Transdermal Patches

To maximize the delivery efficiency as well as the convenience of use, several designs have been invented to fabricate transdermal patches. Schematic illustrations of various important types of transdermal patches are shown in **Figure 3**.

As shown in **Figure 3a**, for single-layer drugs in adhesive patches, the drug to be delivered is dispersed in a single layer of polymeric material with adhesive properties.^[48] A backing laminate made of impermeable materials is placed below the single layer. The drug is released from the laminate layer that supports the single polymer layer containing the drug. An example of this type of transdermal product is Daytrana transdermal patch that contains the drug methylphenidate. **Figure 3b** illustrates the multi-layer drug in adhesive skin patches. A drug reservoir layer is placed between a temporary protective layer and a permanent backing layer for the controlled release of the drug over an extended period of time up to a maximum of seven days. Drugs for smoking cessation and hormone therapy are delivered using multi-layer skin patches.^[49] In the vapor transdermal patches, the drug is dispersed in a single-layer adhesive polymer that releases vapor at a controlled rate. Introduced in 2007 in Europe, Nicoderm CQ are vapor transdermal patches

containing essential oils and are used to help quit smoking habits. Similar essential oil-containing patches are available for pain-relief and decongestion.^[50] In the membrane-based reservoir patches, a reservoir of the drug is placed between an impermeable backing layer and a polymeric membrane (porous). The polymeric membrane is usually made of a hypoallergenic adhesive polymer such as copolymers of ethylene vinyl acetate, and this membrane allows the controlled release of the drug from the reservoir.^[51] Some commercial transdermal patches of this type are, Transderm-Nitro (containing nitroglycerin), Transderm-Scop (containing scopolamine), and Catapres (containing clonidine). Micro-reservoir transdermal system is a combination of matrix-dispersion and reservoir system (**Figure 3c**). The drug to be delivered is suspended in an aqueous solution of water-soluble polymer followed by homogenous dispersion in a polymer matrix (lipophilic). The homogeneous dispersion is achieved by mechanical shear force. This leads to the formation of a large number of microscopic spheres that act as the drug reservoir. The polymer matrix is formed through chemical crosslinking to attain thermodynamic stability of the drug dispersion.^[52] Other FDA-approved transdermal patches can be categorized as matrix-type delivery systems, including adhesive tapes, transdermal spray and gels, iontophoretic delivery, and phonophoresis delivery.^[53] The key transdermal patches and the type of system are listed in **Table 3**.

3.3. Structural Composition of Transdermal Drug Delivery System

Transdermal drug delivery system or patches consists of the following components: polymer matrix, drug, permeation

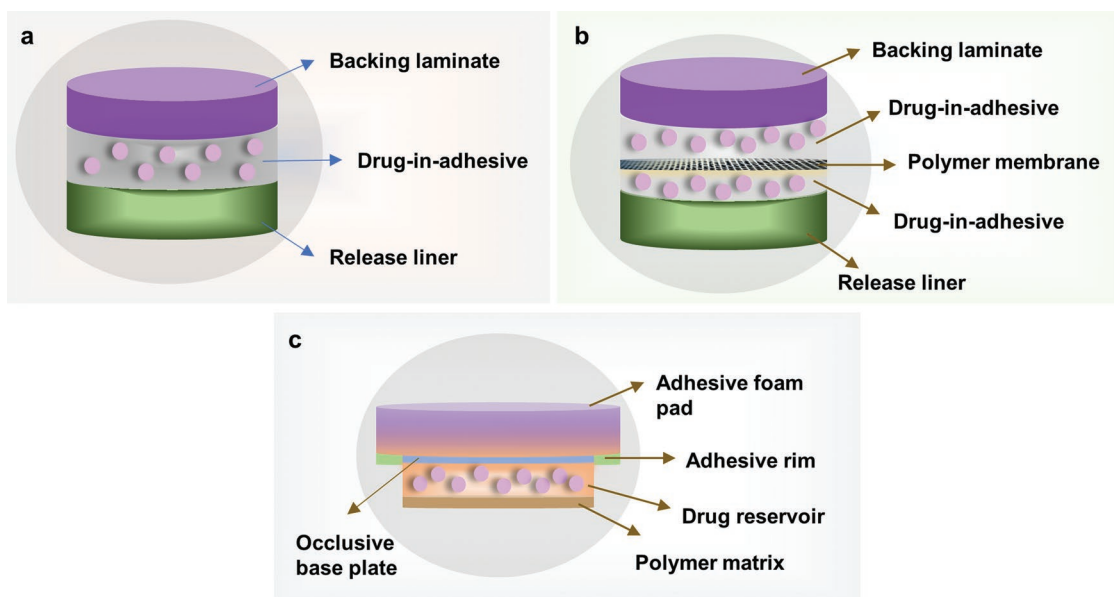


Figure 3. Schematic illustration of various types of transdermal patches. a) Single-layer drug-in adhesive system, b) multi-layer drug-in adhesive system, and c) micro reservoir system.

enhancers, pressure-sensitive adhesives, backing membrane, release liner, and other excipients. In this sub-section, we summarize the materials of each component to fulfill the requirements for high transdermal efficiency.

3.3.1. Polymer Matrix

In the transdermal patch, the rate of drug release from the drug reservoir can be controlled by the polymer matrix that receives much attention in constructing the patch. Microporous copolymers of polypropylene and ethylene vinyl acetate (Alza Corporation), silicone rubber (Searle Pharmacia), ethyl cellulose and isosorbide dinitrate (Sigma), hydroxypropyl methylcellulose (Colorcon) are well-known components of transdermal patches for the controlled release. The selected polymers should be biocompatible with the skin as the critical criterion for designing transdermal patches.^[63]

Both natural and synthetic polymers are used in transdermal patches. The natural polymers can be hydroxypropyl methylcellulose, sodium carboxymethylcellulose, cellulose acetate,

methylcellulose, ethylcellulose, sodium alginate, chitosan, gelatin, and sodium carboxymethyl guar.^[64] The synthetic polymers include poly(ethylene glycol), polyvinyl alcohol, polyvinyl pyrrolidone, silicon rubber, methyl methacrylate, and ethyl vinyl acetate.^[65]

3.3.2. Drugs

Several physicochemical properties of drugs are considered for transdermal delivery. The ionization of functional groups (pH dependent) and hydrophobicity of the drug molecules are the two essential properties that influence skin penetration and diffusivity.^[50] Other important physicochemical properties include melting point, molar mass, partition coefficient, and concentration gradient. Also, the solubility of the drug in water and in oil should be ideally greater than 1 mg mL⁻¹. For instance, lipophilic drugs with low to moderate molar mass (less than 1000 g mol⁻¹) (e.g., Fentanyl) have been employed in transdermal patches.

Table 3. Transdermal patches and types of system.

Type of system	Polymer matrix	Drug	Ref.
Matrix	Hydroxy propyl methylcellulose	Propranolol	[54]
Matrix	Silicone elastomers	L-Timolol maleate	[55]
Matrix	Ethyl cellulose	Isosorbide dinitrate	[56]
Gel	Hydroxy propyl methylcellulose	Hydrocortisone	[57]
Drug-in-adhesive	Acrylics	Tacrine	[58]
Drug-in-adhesive	Cariflex	Dihydroetrophine	[59]
Drug-in-adhesive	Acrylic/silicone polymer	Diclofenac diethylamine	[60]
Reservoir	Hydroxy propyl methylcellulose	Nicorandil	[61]
Membrane moderated	Hydroxy propyl methylcellulose	Nimodipine	[62]

3.3.3. Permeation Enhancers

The first barrier of the skin is the stratum corneum. Chemical permeation enhancers are chemical compounds that weaken the barrier properties of the stratum corneum by disrupting the ordered intercellular lipid bilayers. This disruption decreases the barrier resistance and enhances the permeation of drugs into the systemic circulation via the skin.^[66] An ideal enhancer should be inert, non-toxic, non-allergenic, non-irritating, and compatible with drugs and other excipients in the transdermal patch. To date, about 360 chemical compounds have been identified as chemical permeation or penetration enhancers that work through different mechanisms. Some mechanisms of action are i) solubilization of lipids within the stratum corneum, ii) hydration of the stratum corneum, and iii) increasing the fluidity of lipids (intercellular) in the stratum corneum.^[67]

Examples of chemical permeation enhancers are ethanol (the most common), essential oils and terpenes (cineole, carveol, citral, linalool, menthol, d-limonene), sulfoxides, fatty acids, surfactants (sodium lauryl sulfate, tweens, and pluronic), urea, bile salts, and urea.^[68] Physical permeation of stratum corneum can be achieved by microneedle-based devices, skin abrasion, skin puncture and perforation, iontophoresis and electroporation, suction ablation, and needless injection.^[69]

3.3.4. Pressure-Sensitive Adhesives

The success of transdermal patches or devices depends on the adhesive characteristics of the patch. For efficient delivery of drugs, the patch should be completely in contact with the surface of the skin, through inter-molecular attractive forces between the patch and the skin.^[70] The pressure-sensitive adhesives are viscoelastic materials (polyisobutylene, materials based on silicone and acrylic acid) that adhere to the skin with little applied pressure (finger pressure). Specifically designed PSA generally do not require solvent, water or heat to activate the adhesive, which is highly dependent on the amount of applied pressure.^[71] The advantages of PSA include high compatibility with the attaching materials, short assembly time, low cost, and elimination of the need for surface refinishing. However, these adhesives are difficult to clean due to the strong peel adhesion and shear resistance (cohesion) that may damage the skin when removed.

3.3.5. Release Rate Controlling Membrane

The rate of diffusion of the drug from the transdermal patch can be controlled by an inert matrix membrane such as ethylene vinyl acetate (EVA), polyurethane, polyester-polypropylene, aluminized plastic laminate and silicone rubber. By altering the composition, thickness and porosity of the rate-controlling membrane, the drug dosage per area of the patch can be precisely adjusted.^[72] The drug can be in the form of a solution, suspension, or gel or dispersed in a polymer matrix that stabilizes the drug in this micro-reservoir system. The outer side of the membrane is often adhesive, thin, drug-compatible, and hypoallergenic to permeate the drug delivery

by zero-order release rate. Thus far, the rate of drug release for this type of TDDS patch is predictable and stable upon contact with the skin, especially by the surface moisture.^[70] Although the membrane is stable for controlled release, it can be further integrated with smart-responsive functionality to meet the physiological requirement of the drug dosage on demand.

3.3.6. Release Liner

Release liner is a protective liner and part of the primary packaging for transdermal patches, which is removed before the application of the patch on the skin. It consists of a base layer that may be non-occlusive (fabric of paper) or occlusive (fluoropolymers, linear fluoroacrylates, polyvinylchloride, and polyethylene).^[73] Hence, it does not come into direct contact with the skin but in direct contact with the drug permeation layer. Thus, the chosen materials must be chemically inert, have limited permeation to the drug, and have a low affinity toward water.^[74] However, cross-linking is often formed between the adhesive and the release liner before usage and an unacceptably strong force may be required to remove the liner (e.g., Scotchpak 1022 and Scotchpak 9742, 3 M Drug Delivery Systems, St. Paul, MN, USA).^[75]

3.3.7. Backing Laminate

This inert membrane facilitates oxygen and moisture transmission across the transdermal patch. The backing material prevents the leaching of other additives from the patch into the skin and has low water vapor transmission rates to increase the hydration and permeability of the skin. Silicone oil, EVA, 3 M Scotchpak Backing 1006, polyisobutylene, polypropylene resin, and polyethylene are some important examples of materials used as backing laminates in transdermal patches.^[76]

3.3.8. Other Excipients

A solvent such as water, ethanol, isopropyl myristate, isopropyl alcohol, acetone, or dichloromethane is either used alone or in combination to develop the drug reservoir. The plasticity of the transdermal patches can be tuned by adding plasticizers (concentration range 5–20%), including triethyl citrate, and dibutyl phthalate, glycerol, phosphate esters and propylene glycol.^[77] Cosolvents such as propylene glycol and ethanol are added along with permeation enhancers to promote drug diffusion.

3.4. Recent Advances in Transdermal Patches for Drug Delivery and Wound Healing

Apart from mechanical constraints, hydrogel-based transdermal drug delivery patches have been captivating for non-invasive drug administration for patients. The previously described hydrogel structure composed of the backing layer and adhesive layer provides a convenient application procedure for transdermal drug delivery, especially for drug-in-adhesive

patches. As mentioned above, Kim et al. reported PAM-PDA based adhesive hydrogel patch incorporating extra-large pore mesoporous silica nanoparticles that encapsulate a model drug, Rhodamine 6G.^[22] This study demonstrates the importance of fabricating nanocomposite polymers as an effective biopatch, hydrogel glue, and TDD system. Besides the inorganic nanomaterials, extracellular vesicles (EVs) are membrane vesicles with diameters of 30–5000 nm secreted from different types of cells showing the ability to treat disease because they contain a collection of useful biomolecules, including microRNAs (miRNAs).^[78] Vunjak-Novakovic and colleagues recently developed a type I collagen-based hydrogel patch formed within a gel-foam mesh to entrap and retain delivering induced-pluripotent-stem-cell-derived EVs (iCM-EVs) that showed high therapeutic potentials to treat infarcted hearts (Rat model of acute myocardial infarction, left anterior descending artery ligation) by providing protection from injury and by promoting recovery after injury (Figure 4a).^[79] Their results showed that the hydrogel patch sustainably released 3×10^{10} EVs over 21 days in vitro and the implantation of the hydrogel patch onto the rat myocardium resulted in significantly reduced infarct size, pathological hypertrophy and apoptosis. Their findings suggest the possibility of employing wearable hydrogel patch percutaneous approaches to treat myocardial infarction.

Wound healing of the skin is a prolonged process comprising hemostasis, inflammation, proliferation, and remodeling.^[81] Numerous factors can hinder the healing process, including infections, aging, and ischemia disease.^[82] For instance, diabetes is known to impair wound healing, leading to chronic wounds, such as diabetic foot ulcers (DFU), which makes the wound challenging to recover even for a long period of time. The existing wound dressings and bandages only provide physical coverage and limited capacity for absorbing wound fluids, with the lack of capabilities to form rapid and robust adhesion on wet wounded skin (e.g., DFU). These restrictions ultimately slow down wound healing. In order to prevent chronic wounds, it is highly desirable to design advanced wearable patches that can speed up wound closing. Functional hydrogels have emerged as a propitious biomaterial for addressing this issue in replacing convectional fibrous and absorptive dressing.

Physical or biochemical stimuli-responsive materials have been an active area of research for the diagnosis and bio-regulation of cellular behaviors.^[83] Among the possible type of stimuli, pH level in the wound bed is a critical indicator for evaluating the wound healing progress. In particular, healthy skin or acute healing wounds shows a slightly acidic environment, ranging from pH 4 to 6, while chronic wounds are more alkaline, with pH ranging from 7.3 to 10. This pH variation provides insight into developing pH-controlled transdermal drug delivery in hydrogel patches for accelerating wound healing. Ziaie et al. demonstrated a pH-actuated hydrogel to dispense antibiotics from an array of mm-scale pumps to treat bacterial-infected chronic wounds (Figure 4b).^[84] Each hydrogel subunit consisted of poly mAA-co-AM gel, prepared by mixing two pre-gel solutions, methacrylic acid (mAA) and AM. This poly mAA-co-AM gel could swell at high pH and develop high hydrostatic pressure to push against the thin polydimethylsiloxane (PDMS) membrane and facilitate the antibiotic release from the drug reservoir to the drug outlet (Figure 4c). Their results illustrated that a single cell of the fabricated pump achieved constant flow

rates as small as $<0.1 \mu\text{L min}^{-1}$ over 4 h at backpressures of up to 8 kPa over 40 mm² spatial coverage at pH 6 to 10 and maintained a zero-delivery rate at non-infected regions (pH < 6). This device was also shown to work under normal daily activity for up to 12 h and effectively induced 58 times decrease of live *Pseudomonas aeruginosa* after 24 h pH-triggered antibiotics treatment. This study highlights the possibility of incorporating other types of stimuli to achieve a broad range of biomarker-based treatments.

A recent breakthrough reported by Zhao et al. developed a strain-programmed patch that showed rapid, and robust wound adhesion and promoted diabetic wound closure (Figure 5a).^[85] This patch was composed of two layers: 1) a non-adhesive elastomer backing based on hydrophilic polyurethane and 2) a bio-adhesive layer based on crosslinked networks of poly(acrylic acid) grafted with *N*-hydroxysuccinimide ester (PAA-NHS ester) and chitosan as the layer for double skin bioadhesive effect (dry and hydrated adhesion) via physical (hydrogen bonds between skin surface chemistry and poly(acrylic acid) networks) and covalent (NHS ester with primary amino groups of the skin surface) crosslinking mechanism (Figure 5a). Importantly, the authors programmed the strain in the patch by pre-stretching the assembly of the hydrated bioadhesive layer bonded with the elastomer backing along in-plane directions (anisotropically strained programmed patch) by a confined ratio (Figure 5b) and maintained this pre-stretch until this layer being dried to the glassy state (dry state). Critically, the rigid elastomer backing refrained this pre-stretched bioadhesive from relaxing. Next, the application of the patch on wet wounded tissues induced a rapid (only 5 s) and robust adhesion to the tissue surface via the as-mentioned mechanism when absorbing native physiological fluids and/or moisture from the wet wounded tissue. This hydration caused the hydrogel patch to return to the soft rubbery state from the glassy state within 30 s by releasing the programmed strain along the in-plane direction, thereby generating contractile stress to mechanically facilitate the closure of the wound (Figure 5b). Furthermore, the addition of detachment solution to the hydrogel broke both physical and covalent crosslinking at the tissue interface (Figure 5a), indicating the capability of on-demand removal of the patch upon wound dressing changes. This study demonstrated the important concept of the hydration-based shape-memory mechanism to promote wound healing in a highly predictable manner.^[85] The authors further applied this patch to the excisional wound model of male db/db mice, ex vivo human skin (28 to 41 years old female skins from a commercial vendor, BioIVT), mini pigs (Yucatan miniature swine, Figure 5c) and humanized mice (homozygous *Foxn1tm*, Jackson strain no. 002019) that all showed much better re-epithelialization, angiogenesis, and pro-regenerative phenotype than those by conventional wound dressings or the same hydrogel patch without strain-programming for wound healing. These findings imply the feasibility of strain-programmed patches to treat other forms of acute and chronic wounds.

3.5. Multifunctional Hybrid Patches

In recent years multifunctional and multicomponent hydrogel materials have gained importance in transdermal drug delivery

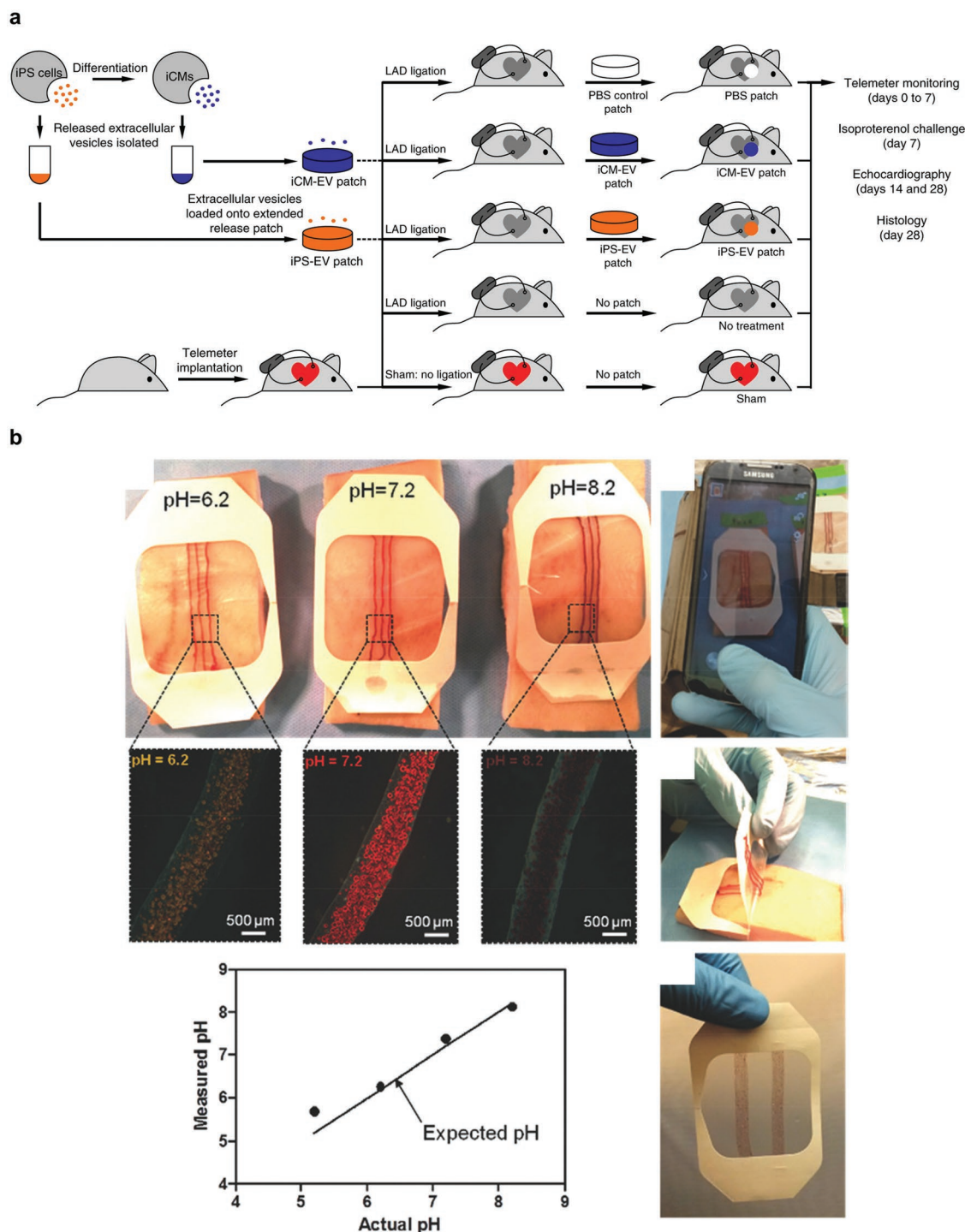


Figure 4. Representative work of recent advances in hydrogel patch-based transdermal drug delivery system. a) Type I collagen-based hydrogel patch for extended delivery of iCM-Evs to treat myocardial infarction. Reproduced with permission.^[79] Copyright 2018, Springer Nature. b) A flexible pH-sensing hydrogel fiber for probing the pH of chronic wounds. Reproduced with permission.^[80] Copyright 2016, Wiley-VCH.

systems. This is because, specific properties can be tailored for sustained and effective delivery of drugs. The benefits of these materials in transdermal drug delivery are, i) the sustained release of drugs over a long period of time, ii) on-demand interruption of drug delivery (the device or patch can be removed

easily), and iii) the hepatic first-pass metabolism can be bypassed. In addition, the hydrogel materials, due to their high-water content, provide a healthy environment for the skin. Copolymer hydrogels based on polyethylene glycol (PEG) and bovine serum albumin (BSA), with its high water content of

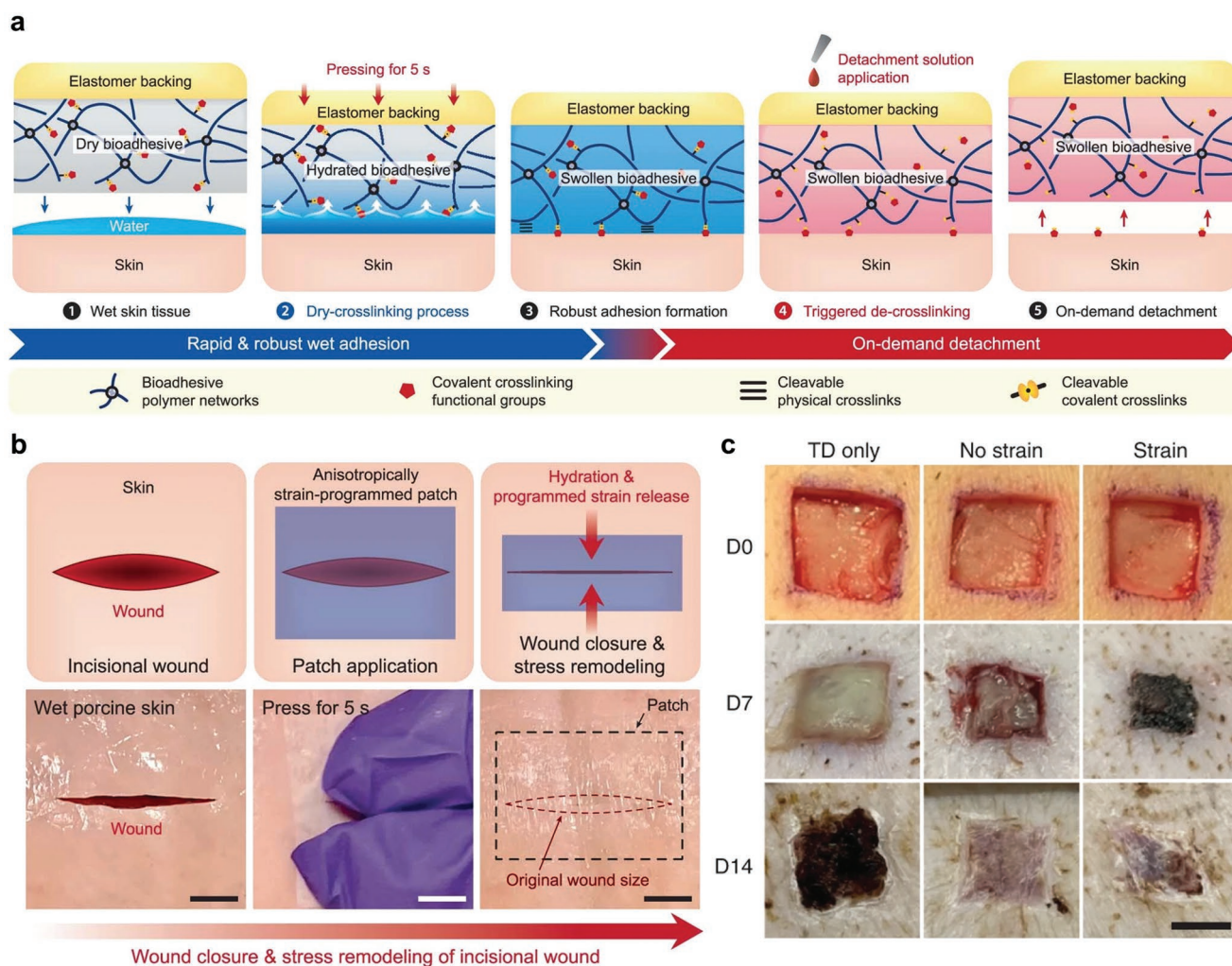


Figure 5. A recent representative wearable hydrogel patch, a strain-programmed patch for diabetic skin wounds. a) Schematic illustration of the working mechanism. b) Closure of an incisional wound on porcine skin by the patch. c) Representative images of the porcine wound before and after the strain-programmed patch applications, macroscopic and microscopic wounds at different time points post-treatment. Reproduced with permission.^[85] Copyright 2022, Springer Nature.

96% have been used as transdermal hydrogels in the delivery of hydrophilic and hydrophobic drugs.^[86] The transdermal system based on copolymers of alginate and Pluronic F127 has shown good skin permeation levels.^[87] Several other multi-component systems with good properties have also been developed for the subcutaneous delivery of drugs, and these include crosslinked poly(hydroxy ethyl methacrylate) with cysteine, poly(acrylamide-monomethyl itaconate), and poly(acrylamide-monopropyl itaconate).^[88] These materials provide minimal mechanical irritation and broad acceptability of drugs with different molar masses. Many multi-component hydrogel products for transdermal drug delivery and wound dressing are currently available in the market. A few important ones are given below, along with the name of the manufacturer, Aquatrix II (based on polyvinyl alcohol and Chitosan, Hydromer Inc.), Smart Hydrogel™ (based on poly acrylic acid and poly oxyethylene glycol, MedLogic Global), Dermaseal-allergen blocker (based on hydroxypropyl cellulose, Hydromer Inc.), and Corplex™ (based on polysiloxane, polyacrylates, natural rubber, and EVA, Corium International).^[89]

4. E-Skin Patches for Sensing and Health Monitoring

Transcutaneous diagnosis and therapy (theragnostic) including biomolecule measurements,^[90] impedance detection,^[91] drug delivery,^[38,81,92] and electrical biostimulation,^[93] have been prevalently conducted in clinical applications. Nevertheless, traditional electronic devices may not be overwhelmingly suitable for point-of-care (POC) theragnostic, such as wearable electronics that often accompany by bulky electrochemical biosensing machinery or drug delivery systems with a large reservoir to store liquid electrolytes.^[90] These limitations restrict the feasibility of POC and real-time transcutaneous theragnostic for various diseases.

Recent advances in ultrathin and miniature flexible devices employing polymeric devices have been popular due to their excellent flexibility and conductivity.^[78,94] However, typical wearable polymer-based devices cannot fit the irregularity of the skin surface, including microscale wrinkles that result in air gaps between the device and the skin, thereby impeding ideal

conditions of electrical/physical contact for precise biosignal measurement and health condition monitoring.^[95] Moreover, these devices do not possess an effective capacity to store liquid-state ionic molecules, such as electrolytes and drugs, for on-site delivery. The E-skin patches benefit the biosensing or electrical stimulation at the skin surface because of its good and stable adhesion.^[96]

E-skin is made up of stretchable and flexible conductive and substrate material. Typical electrode materials for E-skin are poly(3,4-ethylenedioxythiophene) polystyrene sulfonate (PEDOT:PSS), graphene, carbon nanotubes, and metal nanoparticles, while the generally used materials for the E-skin substrate are hydrogels, ionogels, and elastomers such as PDMS, polyurethane, and silicone rubber. PDMS is the most widely used substrate material because of its significant stretchability, transparency, and biocompatibility.^[97] The availability of limited medical resources for a rapidly rising population has resulted in the massive demand for biomedical devices that can do non-invasive and real-time monitoring of the human body which can be extremely helpful in personalized healthcare. Some of the health monitoring purposes where E-skin is used are discussed below.

4.1. E-Skin Patches for Biochemical Sensing

4.1.1. Sweat Sensors

Fluid secretion from the human body is commonly used to regulate adjusting hemostasis.^[98] For instance, salivary uric acid is a biomarker for various diseases such as hyperuricemia, gout, and renal syndrome, while chloride ions and glucose in sweat is highly related to cystic fibrosis and diabetes, respectively.^[95] Such continuous monitoring provides information to users and medical professionals leading to a well aware of health and better disease management.

Sweating is associated with exercise and high ambient temperature to regulate core temperature during endogenous metabolic or stress processes. Sweat is commonly lost from the human body during physical labor or while working in hot environments and has a key role in processes such as thermoregulation and homeostatic functions (galvanic skin response).^[99] For example, Heikenfeld et al. developed an ultra-simple, low cost, and wearable hydrogel for real-time measuring local sweat volume in a wide physiological range (e.g., pH 4–9 and salinity 0–100 mM) for people during aerobic exercise.^[90e] Analyzing the content of sweat can provide useful information about body physiology, including nerve damage, autonomic and metabolic disorders, and chronic stress. There are three main types of sweat glands which are eccrine, apocrine, and apoeccrine.^[99,100] Although water and NaCl are the dominant ingredients in sweat, it also consists of many other components, including potassium, magnesium, iron, calcium, zinc, vitamin, copper, lactate, urea, bicarbonate, etc. in varying quantities.^[99,101] Using sweat components as biomarkers for diagnosis has garnered huge attention in recent times.

One of the most promising avenues of research is using E-skin for sweat sensing. The steps involved in sweat sensing

are shown in **Figure 6a**. The sweat can in turn provide essential information such as nerve damage, metabolic disorders, stress, etc. Nyein et al. have fabricated electrochemical sensors on flexible PET to analyze human sweat during different activities such as sleeping, reading, eating, and sitting.^[90f] In Parkinson's disease, there is an abnormal flow of sweat which is related to a low concentration of levodopa.^[101c] They developed a multilayer microfluidic sweat analysis patch that accumulated sweat through the skin interface and monitored pH for acid–base disorder, Cl[−] for cystic fibrosis, and levodopa for tracking drug response in Parkinson's patients (Figure 6b).^[90f] This patch used general double-sided adhesive to attach the skin and a hydrophilic film that consisted of two layers: polyvinyl alcohol (PVA) and an agarose-glycerol (AG-GLY), to facilitate sweat uptake (nL min^{−1} cm^{−2} rate of thermoregulatory sweat at rest) into conductive electrodes through a microchannel. Incorporating agarose-glycerol hydrogel and SU-8 reduced the dead volume in order to draw sweat into the channel; therefore, it minimized accumulation volume and reduced lag times.^[90f] Also, the hydrogel can absorb and retain sweat well onto the sensor quickly. In contradiction, without the hydrogel filler, it required more than 2–200 h to fill the sensing well based on the calculation. The size of this patch could fit various locations, including the shoulder, chest, bicep, wrist, abdomen, thigh, leg, and fingers. Their findings demonstrated the functionality of the patch for accurate dynamic sweat analysis that was affected by routine activities, stress events, hypoglycemia-induced sweating, and Parkinson's disease. Hence, this study shows the advantage of a non-invasive manner to precisely probe deep body biomarkers to understand physiological conditions.

Sweat has glucose which can act as a biomarker for diabetes and routine monitoring of diabetes can be done if a glucose sensor is developed.^[104] Lin et al. have developed an E-skin with electrodes deposited in it for non-invasive glucose monitoring where dendritic nanostructures on electrode surfaces are utilized for higher sensing abilities utilizing sustainable catalytic activities.^[105] The sweat sampling is done by iontophoresis, in which pilocarpine is used to stimulate the sweat glands and a small current is applied so that sweat is induced. The sensor displayed long-term stability as the drift observed was minimum for around 20 h.

Yang et al. developed a sensor to analyze the uric acid and tyrosine in human sweat.^[106] Uric acid is linked with cardiovascular disease, type 2 diabetes, and gout while tyrosine concentrations are associated with tyrosinemia and liver diseases.^[107] Graphene was used for sensor electrodes due to their superb capacity to detect a low concentration of ions and the sensors were fabricated by laser cutting.^[106] This is because graphene-based chemical sensors have rapid mobility of electrons, large surface area, and significant current density. The device's performance was evaluated in a subject exercise and a high correlation coefficient was obtained, which showed the promise of this sensor in personalized healthcare applications. Measurement of respiration rate and temperature of sweat was also demonstrated.

Another recent sweat sensor example reported by Zhang et al. demonstrated a PVA/sucrose hydrogel matrix incorporating colorimetric reagents to sense pH, glucose, Cl[−] and Ca²⁺.^[90d] The glucose sensing zone changed from colorless to

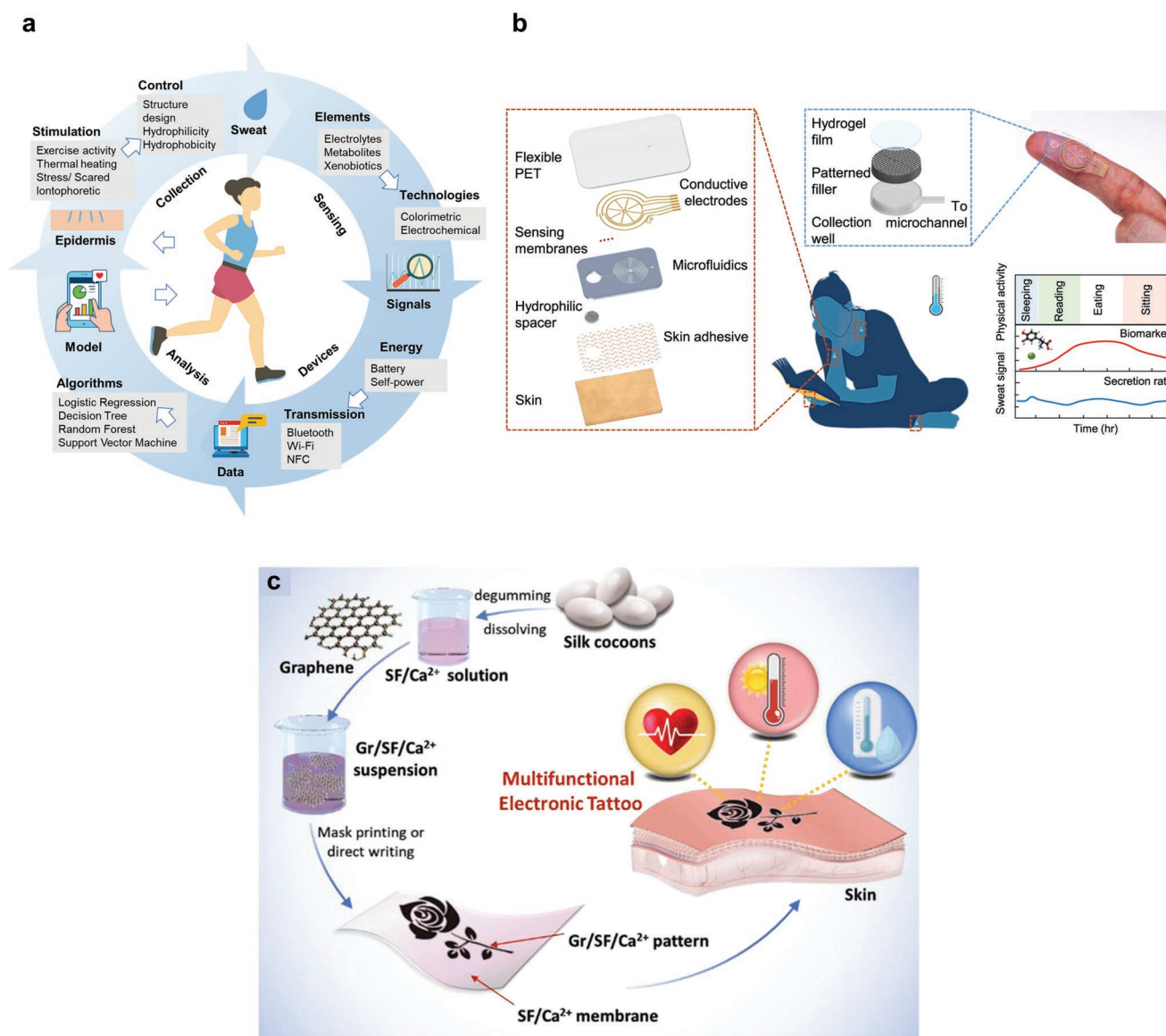


Figure 6. E-skin for sweat and temperature sensing: a) Stages involved from sweat extraction to its monitoring. Reproduced with permission.^[102] Copyright 2022, Wiley-VCH. b) PVA/AG-GLY double-layer hydrogel patch for continuous sweat monitoring. Reproduced with permission.^[90f] Copyright 2021, Springer Nature. c) Graphene/SF/Ca²⁺ E-skin tattoo for temperature monitoring. Reproduced with permission.^[103] Copyright 2019, Wiley-VCH.

pale purple, while the calcium ions sensing zone changed from purple to deep purple. The author used a smartphone to extract RGB signal via an application, Colour Recognizer, and present color information associated with glucose concentration. The PVA/sucrose hydrogel showed repeated and durable adhesion properties on human skin without dislocation during dynamic wrist movement. The hydrogel patch sensor also demonstrated high reliability and stability measurement under mechanical deformation such as rolling, stretching, bending, and twisting. Moreover, it also exhibited fast swelling property, which is essential to sweat sampling.^[90d] A further example of a simple and low-cost sweat sensor was designed by Heikenfeld et al. to measure sweat volume by considering a geometric change of sweat-swelling PAA-PVA hydrogel via a smartphone interface. The patch sweat sensor was optimized for the user with a high

sweating rate of around 100's to 1000's of nL cm⁻² and stable in pH changing environment.^[90e] These findings highlight the recent active area of biofluid sensors with a portable device for detecting signal readouts.

4.1.2. Temperature Sensors

One of the important features of skin is to sense the temperature of an object.^[108] This aspect is particularly helpful in protecting the human from hurting in day-to-day activities as the skin sends a signal to the brain about the temperature and in turn, the brain instructs the muscle to pull the hand back. The application of E-skin can be beyond this sensor actuator coordination. Temperature is also a measure of the health condition

of humans and the development of flexible and stretchable sensors that can adhere to the skin to measure temperature has gathered massive interest.^[108] E-skin that can monitor the temperature of the body is effective in real-time and long-term monitoring and work on this is going on at a rapid pace.^[97] Wang et al. have utilized a self-healing E-skin tattoo made up of graphene/silk fibroin/Ca²⁺ in which healing efficiency is 100 percent in just 0.3s.^[103] The fabrication process for this e-tattoo is shown in Figure 6c. The E-skin displayed high stability and quick response within a temperature span of 20–50 °C and was used to perform long-term monitoring of temperature. The movement of electrons between the graphene nanoplates results in the temperature sensitivity of the E-skin. Luo et al. designed an E-skin made up of MXene and polydopamine-based textiles that showed breathable properties and superhydrophobicity with a contact angle of 151 degrees and used it for long-term analysis of temperature.^[109] Yokota et al. developed a highly sensitive E-skin using a printable positive temperature coefficient thermistor (PTC) that could detect resistivity changes of about six orders with a change in temperature by merely 5 °C and a sensitivity lesser than 0.1 °C.^[110] Jung et al. used conductive printable inks of PEDOT:PSS, thermoelectric material, and silver nanoparticles to develop an E-skin that could monitor temperature within a wide span of around 150 °C.^[111] Oh, et al. developed a temperature sensor made up of poly *N*-isopropyl acrylamide (pNIPAM) hydrogel and polystyrene sulfonate composite with adhesive properties inspired by octopus arms and with thermal sensitivity of 2.6%.^[112]

Some of the temperature detection mechanisms which have been employed include resistive temperature detectors, thermocouple temperature sensors, integrated sensor temperature sensors, and positive and negative temperature coefficients.^[3] Using E-skin for long-term temperature monitoring of the body can be helpful in personalized healthcare.

4.1.3. Pain Sensors

Pain is an undesirable yet inherent part of day-to-day life. The skin of the human body has an interesting ability to sense physical pain that can occur from temperature, collision, or touching a sharp object. Rahman et al. made attempts to create an artificial electronic skin using oxides of vanadium, titanium, and strontium to sense pains for the realization of this purpose via different functionalities, which are thermoreceptors, nociceptor, and Pacinian corpuscle, which work together to mimic the sensory response of human skin.^[113] Pacinian corpuscles are membranes in which fluid is filled and can detect pressure.^[114] The thermoreceptors detect the temperature, while the nociceptors detect the pain.^[113] There are still more complex aspects of pain that are incorporated in this sensor by using the combination of VO₂ and STO-based memristor, where VO₂ is thermally responsive.

4.1.4. Tear Sensors

The eyes are one of the more delicate parts of the human body. In the present time, vision is corrected by using contact

lenses.^[115] The contact lenses can also be used for continuous real-time monitoring of the eyes for the diagnosis of the eye condition. However, contact between a brittle material and an eye can damage the eye. Besides, the use of bulky and opaque material can interfere with day-to-day work.^[116] Thus, it is critical to use sensors made up of soft and flexible materials. Real-time monitoring of the tear fluid can provide physiological information and the advantage of such a sensor lies in the non-invasive mode of operation for an organ as delicate as the eye. The collection of tears can be done non-invasively through processes such as natural secretion or blinking from which the assessment of various biomarkers can be done.^[117] A tear film consists of three different parts: outer lipid, aqueous, and inner mucin, where each layer has its unique function. The outer layer prevents the evaporation of the aqueous solution, which in turn is responsible for the protection of the eye from infection; and the inner mucin acts as an interface between the aqueous layer and the ocular surface.^[118] The key analytes in tear film are glucose, potassium, sodium, magnesium, calcium, chloride, urea, lactate, pyruvate, ascorbate, protein, and dopamine.^[117] A drop of tear has wealth of information in it and several diseases can be diagnosed by the testing of the teardrop. **Table 4** summaries some of the diseases which can be diagnosed by teardrop analysis.

Park et al. have integrated wireless circuits, LED displays, and glucose sensors on a flexible and soft substrate to develop an E-skin for analyzing the glucose levels in tear fluid to check the body for diabetes in real-time.^[116] Chu et al. developed an E-skin contact lens biosensor using Pt and Ag/AgCl electrodes on a PDMS and 2-methacryloyloxyethyl phosphorylcholine (MPC) polymer and found a correlation coefficient of 0.999 between glucose level and the generated output current.^[119] Leonardi et al. developed a wireless contact lens sensor with strain gages to assess the intraocular pressure of pig eyes and the calibration graph showed reproducibility with a confidence interval of 95%, which opens diagnostic possibilities in glaucoma management.^[120]

4.2. E-Skin Patches for Health Monitoring

4.2.1. Human Motion Monitoring

In recent decades, wearable motion sensing has gained tremendous attention for performance enhancement and long-time motion monitoring, especially in sport science and rehabilitation. For example, the measurement of jump height and spiking speed for volleyball players^[121] and tremor frequency for Parkinson's disease.^[122] A wearable motion sensor can detect movement and convert it to useful data for further data processing and analysis. Conventional and commercial components of motion sensors, such as accelerometers and gyro sensors, are rigid and barely skin-adhesive.^[122] It usually requires metal electrodes for conductivity. Hydrogel has been considered as an alternative active material in wearable motion devices because of its ionic conductivity, softness, and well-skin adhesive ability. The hydrogel can serve as electrodes or an electrolyte after ionic enhancement by incorporating conductive materials such as salt or nanocomposites.^[123] An advanced motion sensor

Table 4. Various diseases can be diagnosed by tear sensing.

Disease/Condition ^[17]	Changes in composition
Meibomian gland disease	Proteomic analysis
AIDS	IgA
Ocular Chlamydia trachomatis	IgA, Antichlamydial IgG
Autoimmune thyroid eye disease	Proteomic analysis
Pterygium	α -defensins, and S100 A8 and A9
Keratoconus	Total protein, lactoferrin, and secretory IgA
Ocular rosacea	Matrix metal proteinase-8 (MMP-8), oligosaccharides
Blepharitis	Proteomic and lipidomic analysis, serum albumin precursor, α -1 antitrypsin, lacritin precursor, lysozyme, Ig- κ chain VIII, prolactin inducible protein (PIP/GCDFP-15), cystatin-SA III, pyruvate kinase, and phosphoethanolamine and sphingomyelin for chronic blepharitis
Allergic conjunctivitis	Total protein, serum albumin precursor, Ig gamma-2, leukocyte elastase inhibitor, sPLA2-IIa
Diabetes	Proteomic analysis (glycosylation of the tear proteins, e.g., albumin), glucose
Dry eye (xerophthalmia)	Proteomic analysis, peptide/protein markers (proline-rich protein 4, Mammaglobin B, lipophilin A, calgranulin S100A8)
Sjögren's syndrome	Proteomic analysis, lysozyme, epidermal growth factor, AQP5, IL-1 α and β , IL-6, IL-8, TGF- β 1, IL-1Ra and TNF- α , RNA transcripts for MUC5AC, protein levels of MUC5AC, MUC5AC-positive conjunctival cells, glycosylation of mucins, (GalNAc transferase, GalNAc-T2 and -T6 isoenzymes), O-glycan residues, MMP-9
Glaucoma	Autoantibody reactivities (HSP10, HSP27, MBP, and Protein S100)
Conjunctivochalasis	S100 family (A8, A9, A4), guanosine triphosphate-binding protein 2, L-lactate dehydrogenase A-like 6B, fatty acid-binding protein, keratin type I cytoskeletal 10, glutathione S-transferase P, peroxiredoxin-1, peroxiredoxin-5, and cullin-4B+ glyceraldehyde 3-phosphate dehydrogenase, Pro-MMP-9
Diabetic retinopathy	Proteomic analysis
Lacrimal gland dysfunctions	Proteomic and lipidomic analysis
Cancer	Lacryglobin, actin, albumin
Herpes simplex virus	HSV-specific sIgA, HSV-specific IgG antibodies

was presented by Roy and his co-workers, who integrated the advantages of hydrogel and designed a high-performance synthetic hydrogel (β -CD-g-(pAAm/pHMAM)) for wearable motion monitoring (Figure 7a).^[39] β -CD-g-(pAAm/pHMAM) exhibited stable mechanical properties such as high stretchability in bearing >6000% strain and tensile yield strength of 88 kPa, owing to the reversible hydrogen bonds in the hydrogel matrix. The β -CD-g-(pAAm/pHMAM) hydrogel exhibited an excellent adhesive property on different interfaces owing to the abundant $-\text{CONH}_2$ group, $-\text{OH}$ group, and hydrophobic polymeric backbone. The adhesive strength was quantified by lap shear test such that adhesive strength on wood, skin, and glass was around 50.1 kPa, 34.5 kPa, and 29.3 kPa, respectively. The sensitivity of the β -CD-g-(pAAm/pHMAM) hydrogel was related to the response between the mobility of electrons from functionalities such as $-\text{NH}_2$, $-\text{OH}$ groups in the polymer network and an external stimulus. The hydrogel exhibited a high sensitivity up to 0.053 kPa^{-1} for 0 to 3.3 kPa and a fast response time of around 130–210 ms with stability undergoing 5000 cycles. Thus, these excellent properties turn the β -CD-g-(pAAm/pHMAM) hydrogel into a good flexible pressure sensor for real-time monitoring of human motion. The author further applied the hydrogel to a finger joint to monitor the bending angle at 0° , 30° , 60° , and 90° . The responsible current changes were highly attained and repeatable at each bending angle. The repeatable results suggested the hydrogel exhibited remarkable accuracy, sensitivity, and fast recovery and response.

Previous studies always focus on direct motion monitoring without feedback control. A feedback control system may provide a tailor-made solution to meet individual needs. Wu et al. developed a motion-controlled Poloxamer 407-based hydrogel patch for non-invasive drug release via iontophoresis, which consisted of a vital component triboelectric nanogenerator (TENG), as an energy harvester and a motion detector (Figure 7b).^[124] Poloxamer 407-based hydrogel is stretchable, biocompatible, conductive, thermosensitive, and reversible in thermoregulation at the sol–gel transition temperature. Owing to these properties, this hydrogel has overwhelming advantages as a skin-patch drug release material, such as easy for drug loading, good adhesive on the skin and high ionic conductivity. The study demonstrated a pain-relief drug-release system for ankle injuries in which the drug-loaded patch was attached to the ankle and a TENG was inserted under the shoe. When the patient walked, TENG was activated to generate around 320 nC charge transfer per cycle, 12 μA current and 4 V voltage to the drug-loading patch via wires. These signal outputs were able to drive drug release from the patch. The patch consisted of two isolated hydrogel patches on a PDMS frame, while only one patch was loaded with the cationic drug. Once the electrical signal arrived, the charged drug in the patch flew to another non-drug-loading patch via skin. As a result, drug release via skin was an achievement. The study showed the proof-of-concept that the hydrogel drug release patch was controlled by a body motion in a feedback loop system using an energy

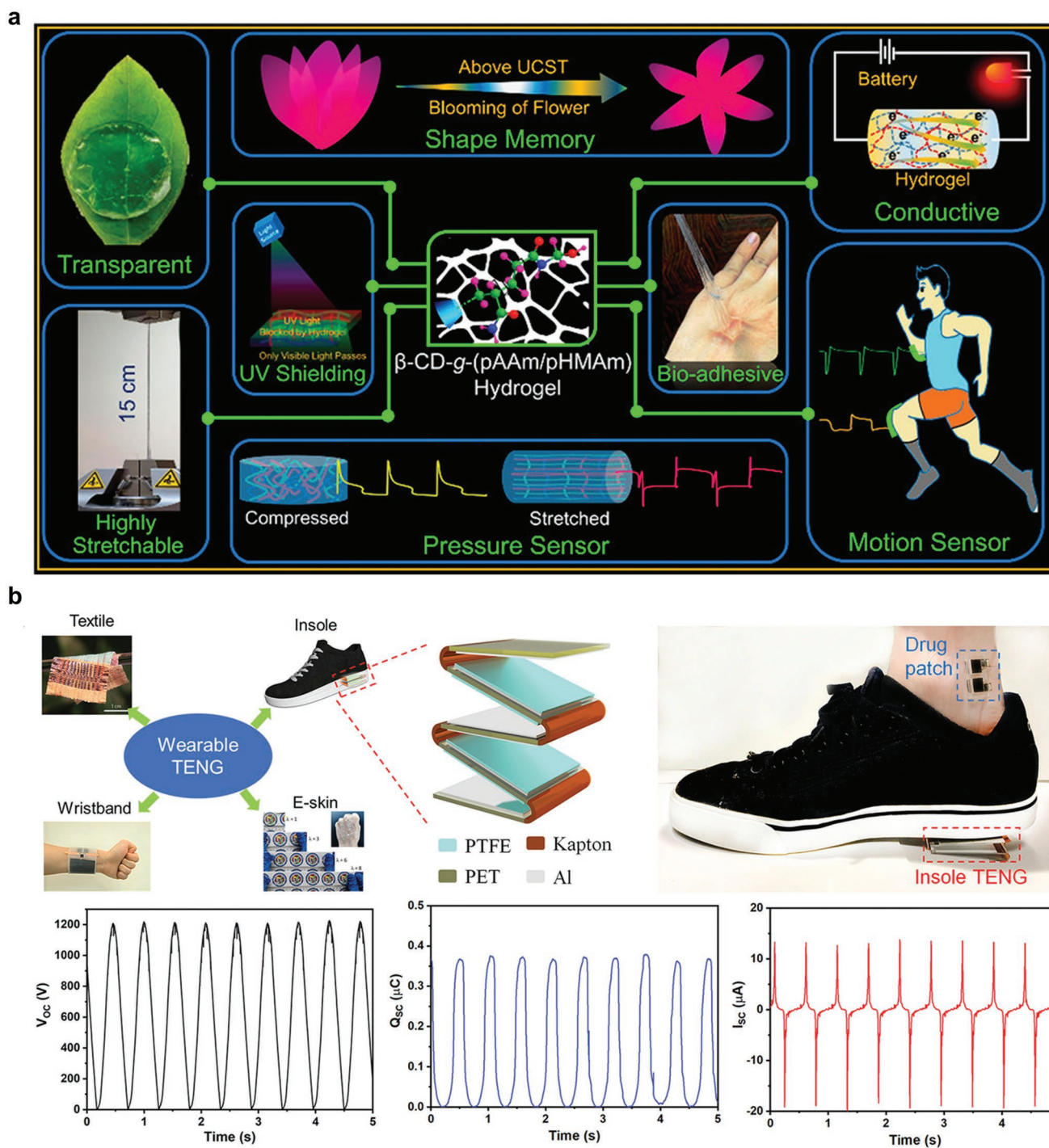


Figure 7. Representative studies on wearable hydrogel patches for motion sensing. a) A self-powered motion detector with poloxamer 407-based hydrogel patch for drug delivery in a feedback controlled by body motion. Reproduced with permission.^[39] Copyright 2020, Wiley-VCH. b) A β -CD-g-(pAAm/pHMAM) hydrogel-based motion sensor. Reproduced with permission.^[124] Copyright 2022, American Chemical Society.

harvester TENG. The authors also applied the system to the pig skin to show that stimulated fluorescence drug such as methylene blue (MB) was successfully administered via skin after a 6-h operation. The finding demonstrates the feasibility of a motion-controlled wearable self-administer hydrogel patch in a feedback-control manner which is also possible to apply for other locations such as the shoulder and elbow.

4.2.2. Energy Harvesting E-Skin

A flexible and stretchable supercapacitor system has emerged as a promising energy storage system to power wearable health and biomedical devices, requiring resistance to bending, stretching, and twisting.^[125] However, electrolyte evaporation and leakage are problematic during mechanical deformation,

resulting in decreasing the supercapacitor lifetime under ambient conditions.^[126] Aqueous electrolytes may encounter electrolyte loss due to evaporation under ambient conditions and electrolyte dissociation. Liquid electrolytes, such as gel electrolytes, were considered to reduce these problems, but their ionic conductivity was inferior to aqueous electrolytes. Conductive hydrogels composed of a crosslink hydrophilic polymer network and incorporating conductive elements such as carbon-based material, salt (such as NaCl, LiCl, and KCl) and metallic nanoparticles.^[123] The physicochemical properties of these hydrogels render them promising in flexible energy storage systems such as supercapacitors and batteries.^[127] Thus, conductive hydrogels are an emerging potential material in stretchable electrodes and electrolytes to resolve poor ionic conductivity, electrolyte evaporation, and leakage issues.

Recently, Yun and Park et al. reported a three-layer stretchable electrochromic supercapacitor of wearable patch devices.^[126] The first layer contained an Ag nanowire working electrode and an Au/Ag core-shell nanowire counter electrode embedded into the PDMS substrate. The second layer is a polyacrylamide (PAAm) electrolyte composed of 1 M LiClO₄ salt in propylene carbonate (PC) was inserted between two electrode layers to maintain the electrical conductivity under mechanical deformation such as bending, tensile and stretching conditions. The third layer contained a WO₃ nanotube which was wrapped by a conductive PEDOT:PSS layer and further embedded into PDMS substrate. The ionic conductivity is 265 mS cm⁻¹, which was superior to conventional gel electrolytes such as zwitterionic PPDP gel electrolyte (17 mS cm⁻¹). Moreover, 94% of ionic conductivity and 93% of water content were maintained under exposure to ambient conditions with 30% relative humidity for 16 days after repeated bending/tensile testing. As a result, the PAAm hydrogel electrolyte supercapacitor provided a high ionic conductivity with 265 mS cm⁻¹ and resolved evaporation, leakage, and dehydration problems under mechanical deformations.^[126] Another example of a flexible and durable supercapacitor developed by Liu et al. utilized a double hydrogel network.^[128] The first network was polyacrylamide crosslinked by nanoparticles, while the second network was alginate crosslinked by zinc (II) ions. The double hydrogel network was inserted into two active carbon platforms, forming a supercapacitor with high specific capacitance. The supercapacitor also showed excellent adhesion, electrochemical properties, and outstanding mechanical deformability,^[128] turning it into a feasible energy provider or energy storage for a wearable biomedical sensor such as a motion sensor. These studies imply the feasibility of hydrogel as active material in designing a supercapacitor as a self-power biomedical wearable appliance under various mechanical deformation, which effectively provides a solution for evaporation, leakage, and dehydration issues.

In addition to a hydrogel-based supercapacitor, hydrogel-based triboelectric nanogenerators (TENG) are energy source alternatives for self-power biomedical wearable applications, including smart skin design shown in **Figure 8a,b**.^[129] The smart skin device had multiple layers. The bottom layer was the Ecoflex elastomer layer, the middle layer was PAA hydrogel containing NaCl as a conductive electrode, and the top layer was Ecoflex-ZnS multifunctional layer. When an external

stimulus such as a finger touched on or removed from the top layer, the current was induced in a reversible manner, resulting in an AC current generation. Hence, the magnitude of mechanical stimuli can be quantified with the lowest limit of pressure detection at 0.58 kPa, which was highly desirable for generating a sense of touch. Remarkably, the smart skin device demonstrated high stretchability with a strain of 700% and Young's modulus of 51 kPa while the functionality of the smart skin device was preserved. Moreover, the PAA-based TENG generated an output voltage of up to 180 V with a peak output current of 65 μA and a maximum power density of 625 μW cm⁻² at an external loading (10 MΩ), showing a desirable performance of harvesting mechanical energy to electrical energy. The author further applied the smart skin device on a human arm, demonstrating that the smart skin device effectively harvested energy and generated a sense of touch steadily.

Jing et al. suggested a dual-electrode hydrogel-based TENG with high power output for wearable devices.^[131] The TENG consisted of two layers separated by an air gap, namely, a tribopositive layer and a tribonegative layer. A tribopositive layer contained a thermoplastic polyurethane (TPU) layer and a PAM layer wrapped by a polyethylene terephthalate (PET), while a tribonegative layer composed of a thin PDMS layer and PAM hydrogel wrapped by PET as well. Polyethylene terephthalate (PET) films were used to enhance mechanical stiffness and quick recovery after compression. The PAM hydrogel was incorporated with NaCl for enhancing ionic conductivity and as dual ionic electrodes. Notably, benzophenone (BP) modification was used to facilitate interfacial bonding between hydrophilic PAM hydrogel and hydrophobic TPU as well as PDMS, leading to 12 times stronger tear strength. The system generated current flow when TPU and PDMS layers were in contact due to potential differences, while separating these two layers caused a reverse current flow in an external circuit. The author applied 6 N force at 10 Hz to generate an output voltage of up to 311.5 V, an output current of 32.4 μA, and a maximum power density 2.7 Wm⁻² at an external loading (4.7 MΩ). The result showed a desirable voltage and current generated by hydrogel material. Owing to its excellent deformative properties, the hydrogel-based energy harvester was highly desirable in developing motion sensors. Xu et al. demonstrated an example that a PVA-hydrogel-based TENG could be an energy provider which harvested mechanical energy from body motions such as bending and a motion detector itself (Figure 8c).^[130] The PVA-TENG was composed of two layers. The top layer contained a hemispheric PVA hydrogel encapsulated by PDMS film and an Ni electrode, and the bottom layer was a flat Al electrode. When the PVA-TENG exhibited an external force, such as bending from human motion, the contact area between the hemispheric PVA hydrogel with PDMS coating and Al electrode changed; thereby inducing differential current movement. The PVA-TENG also attained a relatively high output voltage of up to 200 V and an output current 22.5 μA. The author further applied the PVA-TENG as a motion detector on the elbow joint, which effectively monitored voltage changes from 3.5 V, 12 V, to 16 V for three bending angles 30°, 90°, to 150°, respectively. Moreover, the bending rate is proportional to the open-circuit voltage. For instance, the bending rate increased from 0.6 to 2 times s⁻¹ when the voltage also increased from

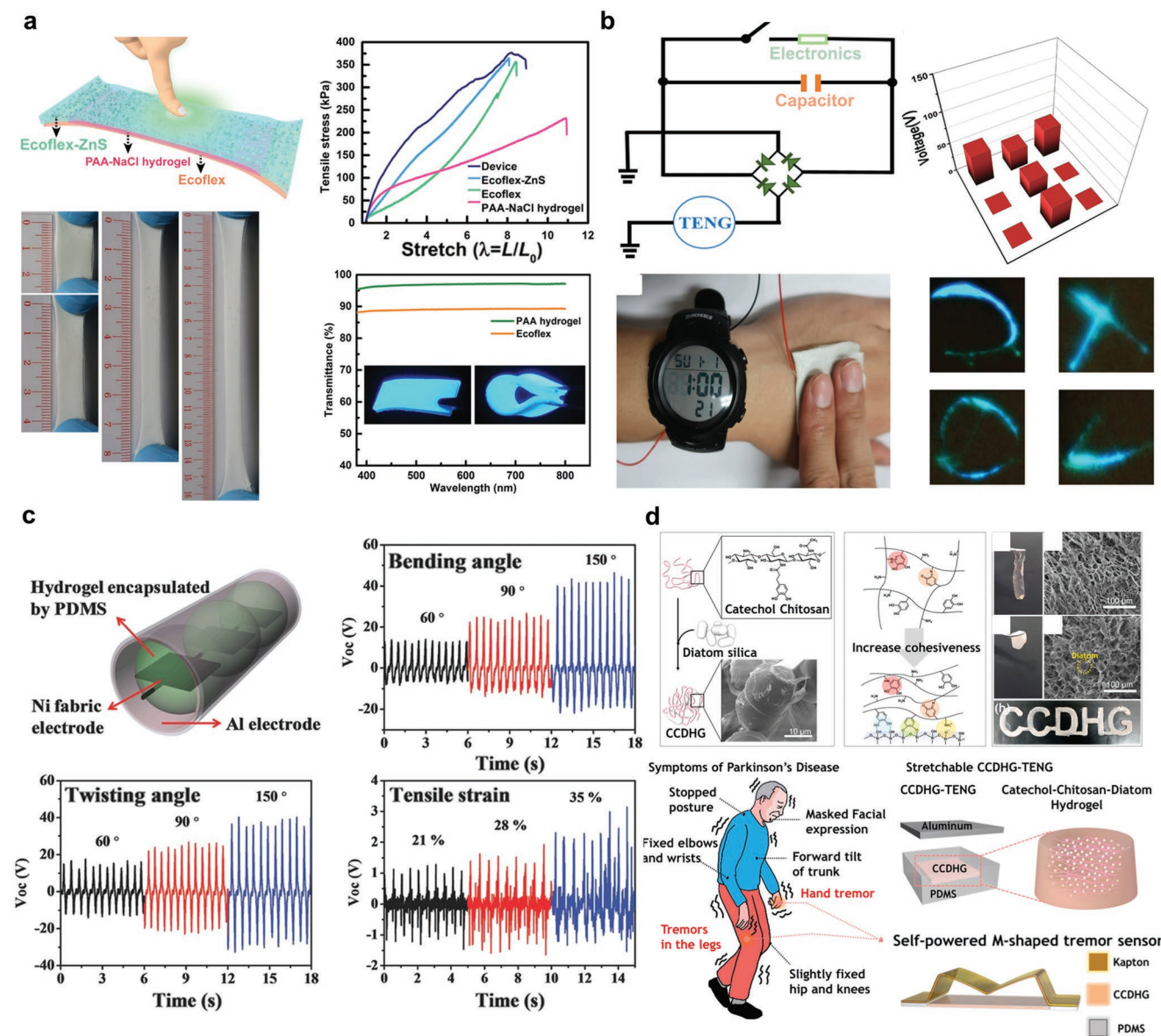


Figure 8. Representatives works of recent advanced wearable hydrogel patch as an energy harvester for biomedical applications. a, b) A stretchable hydrogel-based TENG in smart skin design. Reproduced with permission.^[129] Copyright 2019, Wiley-VCH. c) A PVA-based TENG for energy harvesting and motion sensing device. Reproduced with permission.^[130] Copyright 2017, Wiley-VCH. d) A low-frequency motion sensor by developing CCDHG-based TENG for Parkinson's disease. Reproduced with permission.^[122] Copyright 2021, Elsevier.

3.7 to 17.5 V at the same bending angle. These results indicated the PVA-TENG could quantify the motion movement linearly and undergo bending and other mechanical deformation, such as stretching and twisting, without an external power source. These findings highlight the recent active research interest in developing a hydrogel-based energy harvester with highly flexible and stretchable properties for applied force quantification from human motion.

Kim et al. reported a tremor sensor utilizing catechol-chitosan-diatom (CCDHG) hydrogel-based TENG for Parkinson's disease.^[122] (Figure 8d) The CCDHG-TENG consisted of an Al electrode that was attached to the conductive CCDHG hydrogel with PDMS coating. The working mechanism was

similar to the aforementioned TENG developed by Jing et al.^[120] that an AC current was induced in a contact-separating manner. An 8 N compression force and a mechanical shaker at 3 Hz was used on CCDHG-TENG to stimulate tremor from Parkinson's patient, resulting in generating a maximum output voltage and current were 110 V and 3.8 μ A, respectively, and the instantaneous power density of 29.8 mW m^{-2} at 100 M Ω external loadings. These electrical outputs suggested a desirable performance of CCDHG-TENG as an energy harvester. An M-shaped Kapton film was attached to the CCDHG-TENG to form a tremor sensor which was attached to the wrist of a Parkinson's patient to collect voltage changes and further process the signal by using a machine learning algorithm. The finding presents

the feasibility of a self-power motion sensor to monitor health conditions for diseases such as Parkinson's disease.

4.2.3. Heart Rates Monitoring

Cardiovascular diseases are one of the most common health problems all over the world and they are monitored using an electrocardiogram (ECG).^[134] The pumping of blood to supply nutrients in the human body is served by the heart and heart diseases are very common and around 30% of the population worldwide dies every year because of cardiovascular disease.^[135] The current approach employs ECG to monitor the heart rate in hospitals. However, this is a short time analysis and can lead to a lack of diagnosis data. Zheng et al. developed a breathable E-skin with moisture-wicking and anti-bacterial properties for continuous long-term monitoring of cardiovascular health. As shown in **Figure 9a**, it consisted of a hydrophilic, hydrophobic, and transport layer with multiwalled carbon nanotubes that resulted in the necessary conductance in the E-skin for measuring the ECG signal.^[132] Eskandarian et al. used a knitting machine to obtain a 3D network made of conductive elastomers that could withstand the strain of more than 200%

and were found to be beneficial in long-term monitoring.^[136] Attempts have also been made to ensure good mechanical properties in E-skin along with conductance through the use of graphene.^[137]

4.2.4. Muscle Response Monitoring

Measuring biopotentials muscular activity supports the study of motion dynamics, such as physical exercise,^[138] remote health monitoring,^[139] and prosthetic applications.^[140] In electromyography (EMG), an electrical signal is measured with the nerve's stimulation to the muscles. Monitoring EMG has far-reaching benefits and can be helpful in sports, neuromedicine, and training.^[141] Several types of E-skin for EMG monitoring have been developed. Since the accumulation of sweat can damage the electrode or can interfere with EMG signals, providing the E-skin with breathable properties can be highly useful.^[134] Yang et al. developed a nanofiber-based E-skin with breathable properties for measuring the EMG signals, consisting of polyurethane, silver nanowires and hydrolyzed polyacrylonitrile.^[142] Xu et al. have developed an E-skin consisting of electrodes of gold/copper patterned on silicone

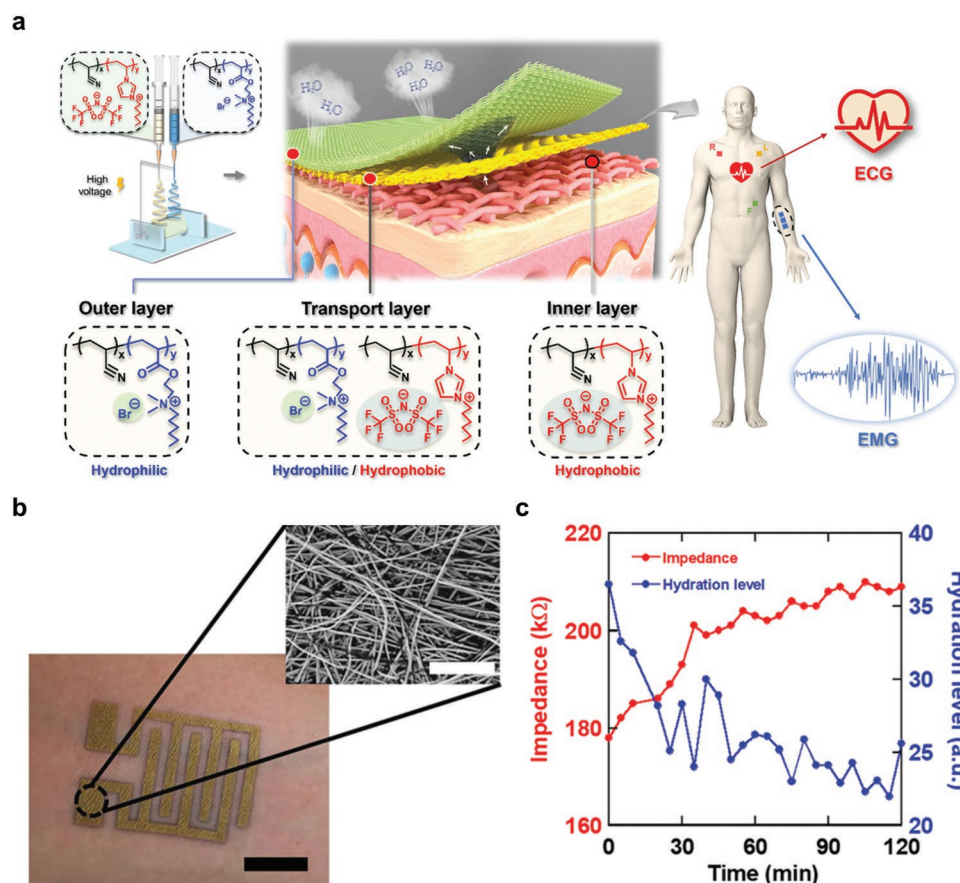


Figure 9. Skin adhesive patches for health monitoring. a) E-skin with hydrophobic and hydrophilic hydrophobic that can be used for assessment of heart rate. Reproduced with permission.^[132] Copyright 2021, Wiley-VCH. b) E-skin with nanomesh electrodes for monitoring skin humidity and c) the temporal change in the skin impedance and the hydration level after application of skin lotion. Reproduced with permission.^[133] Copyright 2020, Wiley-VCH.

elastomer and this device has been utilized for prosthetic control and management of exertion in the lower back.^[143] However, most commercial devices for EMG are based on electronic printed circuit boards (PCBs) that are too rigid and hardly bendable for conforming to soft human tissues for measurement. A stretchable sensing interface ($\approx 20\%$ strain rate^[144]) enables wearability for probing signals from contracting tissues, which can reduce hospital care costs and patient independence. Tavakoli and co-workers recently demonstrated a thin-film stretchable E-skin circuit to interfacing human skin for long-term wearable biomonitoring.^[145] They employed PDMS as the base elastomer for anisotropic conductive composites: silver flakes, carbon black, or silver-coated nickel, which conducted only along the film thickness. Two other types of composites, a tough conductive hydrogel (PAAm-alginate) and silicone-based adhesive gel (Silbione RT 4717) were further coated on the PDMS substrate and stretchable biphasic Ag-In-Ga (silver-eutectic gallium indium alloy) electrodes to formulate a self-adherent patch. The authors compared the biosensing performance of these electrodes with the gold-standard Ag/AgCl and stainless steel electrodes. As a result, Ag-In-Ga and hydrogel electrodes exhibited the first- and second-highest EMG signal-to-noise, respectively, compared to other groups. The ionic environment and the liquid phase interface of the hydrogel electrode facilitated the passage of biopotentials from the human body to the acquisition system. Besides, only the hydrogel electrode showed good reusability depending on the re-absorption of an ionic solution and long expiry duration (>1 year). These findings outline the signature of hydrogel-based conductive as an environmentally friendly and cost-effective electrode with high biosignal recording performance for the future biomonitoring systems.

4.2.5. Electrooculographic Signal Monitoring

Human-machine interactions, soft robotics, and virtual reality/augmented reality have emerged as wireless remote control.^[146] These techniques offer noncontact measurements and long-distance operations for various applications. In electrooculography (EOG), an electrical signal between the cornea and retina of the eye is monitored and has been used in diagnostics of mental disease and in visual navigation, etc.^[134,147] The advantage of EOG is that signal can be analyzed more readily because of its linear nature and the EOG signal is more stable than EMG.^[134,148] In order to prevent damage to the skin around the eye, the EOG electrodes need to be flexible and soft. A graphene based E-skin, developed by Ameri et al. for EOG in the graphene, was fabricated by chemical vapor deposition, and the graphene layer and transferred to the human skin through tattoo paper.^[149] As a result of the substrate free nature, the E-skin was found to have great conformability with the skin around the eye and signal to noise ratio was 15.22 dB, and an angular resolution of 4 degrees was found. Hsieh et al. synthesized a soft skin with a conductive network of silver and polyamide with a sponge package that led to breathability as well as long-term stability in the signal.^[150] Dong et al. developed a soft multifunctional E-skin with the copper film deposited on a PDMS substrate and utilized it for the detection of eye movement.^[151] Recently, Sun et al. developed a highly stretchable

hydrogel wearable patch integrating starch from lotus rhizome as hydrogel skeleton synthesized via sol-gel transition and sodium chloride as electrolyte for EOG signals acquisition.^[152] This hydrogel showed excellent stretchability (790%) and good softness (4.4 kPa) that were superior to most existing pure polysaccharide-based hydrogels. Moreover, this hydrogel demonstrated high conductivity (10 S m^{-1}), good reproducibility (>100 cycles), good linearity ($\approx 300\%$), and strong skin adhesion with high biocompatibility and biodegradability. The author further utilized their hydrogel to measure EOG signals to track the eyeball movement directions that were processed as the digital signals to successfully command the control in a video game (Retro snake). This study shows a great success of a wearable hydrogel patch in mediating EOG signals for noncontact connection between humans and machines.

4.2.6. Electroencephalogram Recording

An electrophysiological signal is monitored in electroencephalography (EEG) to study the state of the human brain and is found to be extremely useful in examining mental health, sleep, and fatigue.^[134] Generally, scalp electrodes are used for EEG. However, they are not suitable for long-term monitoring. Besides, ionic conductive gels for enhancing the conductance between electrodes and the scalp may lubricate the contact site, leading to dislocation and unstable readouts. Thus, adhesive hydrogels are a good alternate option for electrodes because of their mechanical properties, ionic conductivity, and epidermal hydration effectivity to overcome these barriers. Qiao et al. developed a breathable and high comfort E-skin in which graphene oxide particles were coated on polyurethane nanomesh and this E-skin displayed a high stretchability and could be strained to more than 600% and was able to sustain more than 1000 cycles under extension. Besides, the nanomesh resulted in high quality EEG signal.^[153] Someya et al. reported an on-skin paintable and biocompatible conductive biogel to enhance dynamic adaptability to hairy scalp and conductivity for long-term high-quality EEG recording.^[154] The biogel was synthesized by physical cross-linking between gelatin chains and ionic cross-linking between gelatin chains and citrate ions/NaCl. This hydrogel exhibited temperature dependence of rheological properties for the transformation between viscous liquid and viscoelastic gel for enhancing the conformal contact and mechanical interaction with both non-hairy and hairy skin. The authors successfully employed the biogel with a flexible Ag/AgCl electrode to stably obtain EEG alpha rhythms continuously for 24, 48, and 72 h from human subjects, with a high SNR (36.7 dB) and highly accurate classification of steady-state visually evoked potentials recorded in a virtual reality environment using a convolutional neural network-based algorithm. This study highlights the novel strategy of materials science for advanced EEG monitoring and brain-machine interfaces.

4.2.7. Galvanic Skin Response (GSR)

In GSR, the activities of the sweat gland are monitored to examine the emotional state. The sweat glands which are

primarily concerned with emotional arousal are the eccrine sweat glands, as these glands are supplied with sympathetic nerves.^[155] Emotional arousal is connected with skin conductance such that the increase in arousal leads to an increase in skin conductance.^[156] GSR signal amplitude measurements are found to be correlated to stress, excitement and anger.^[157] In GSR sensors, conducting electrodes, typically Ag/AgCl are placed on two points on the skin at specific locations to obtain a GSR signal, which consists of two components: tonic and phasic. The phasic component of the GSR signal is linked with the emotional arousal circumstances.^[156]

4.2.8. Skin Humidity Monitoring

Skin humidity is one key parameter for the assessment of skin diseases. It also provides information about the metabolic levels in the human body. The E-skin needs to be as breathable as possible to ensure no moisture variations on the skin surface and the moisture conditions of the E-skin are compatible with the bare skin.^[134] Matsukawa et al. realized E-skin with nano-meshed graphene electrodes and used it to measure skin humidity by measuring skin impedance, as shown in Figures 9b and 9c, respectively.^[133]

4.2.9. Multi-Parameter Monitoring

Despite the detection of biofluid, the monitoring of other physicochemical factors can report a comprehensive health status. However, current commercial wearable sensors often detect a single parameter. Recent research has explored the feasibility of integrating both physical and chemical sensors, such as electrocardiography electrodes with lactate or glucose sensors, into a single and miniature wearable device. Recently, Wang et al. presented a conformal, stretchable, and integrated wearable hydrogel sensor for probing blood pressure (BP), heart rate (HR), and the level of glucose, lactate, caffeine, and alcohol (Figure 10a).^[90c] In particular, the authors combined rigid biosensors (Figure 10b,c), ultrasonic transducers (BP and HR monitoring) and soft hydrogel (agarose) biosensors, electrochemical sensors (levels of biomarker detection) into a single wearable sensor with high mechanical resiliency (resisting 200 cycles of 20 stretching strain) and absence of sensor crosstalk (high selectivity). The BP and HR sensors consisted of eight piezoelectric transducers. The biochemical sensor was realized using chronoamperometry for the detection of the hydrogen peroxide product of the glucose oxidase, lactate oxidase, and alcohol oxidase enzymatic reactions and differential pulse voltammetry for the detection of caffeine. Their results showed that lactate, alcohol, and caffeine were detected only in sweat, whereas glucose was monitored only in the interstitial fluid of human research participants (Figure 10d). Together, this wearable device provides a reliable and comprehensive biomarker analysis for human health and paves the way for the next-generation wearable patches capable of hybrid chemical–electrophysiological–physical monitoring.^[158]

4.2.10. Skin Adhesion Patches Integrated with a Wireless Electrical System

The conventional systems of monitoring physiological health have been mainly based upon in-person hospital care, in which there is a lag time between examination and results and have involved the usage of costly equipment.^[159] The recent methods of monitoring deal with instant and uninterrupted testing and personalized health care.^[159c,160] These latest advances are dependent on the integration of biosensors with wireless electrical systems that gives birth to the attractive area of point-of-care diagnostics.^[161] Such devices can extract physiological information from the body in real time and can be connected to cloud platforms and mobile phone apps where data analysis and artificial intelligence algorithms can be run over them so that they can provide meaningful information about health. Furthermore, mobile apps can also be virtually connected to healthcare for advice regarding therapeutic procedures. The integration of biosensors with wireless integration has been shown in the stages shown in biosensing (Figure 6a), where data is transferred to a device through WiFi/Bluetooth/Near Field Communication (NFC) and machine learning algorithms such as regression, supporting vector machine decision tree to obtain fruitful information from the data. For wireless data transmission, Bluetooth and NFC consume lower power, while the power consumption involved in Bluetooth is comparatively more. Thus, NFC and Bluetooth are preferred for data transmission from the sensor to mobile devices.^[159c] Nyein et al. developed an E-skin patch with a printed circuit board that was connected to the mobile device and the data was transferred to the device through Bluetooth.^[162] This device was utilized to analyze the concentration of sodium ions in the sweat solution and for the flow rate of sweat.

In summary, we have discussed the cutting-edge hydrogel-based patches for various applications, including wound healing, drug delivery, physicochemical biosensing, and E-skin for electrophysiological signal monitoring, that are important for improved healthcare of humans. Table 5 summarizes representative examples of different types of hydrogel patches with their types of materials, mechanical properties and adhesion energy/conductivity for different biomedical applications.

5. Conclusions and Outlook

Recent developments in the fabrication of skin adhesive patches are believed to revolutionize clinical translation in reducing patients' complications as well as commercialization for different types of biomedical applications. However, future development of a skin adhesive patch, aiming for a particular application along with commercialization, should satisfactorily meet all the requirements, and researchers must continue to focus their efforts on the following points.

As the skin adhesive patch fabricated from polymeric hydrogels and elastomers can attain a tight fitting as well as a direct interface with the skin, a more innovative and bioinspired adhesion mechanism should be developed that meets all the requirements for developing a biocompatible and long-term attachment to different types of human skin surfaces without

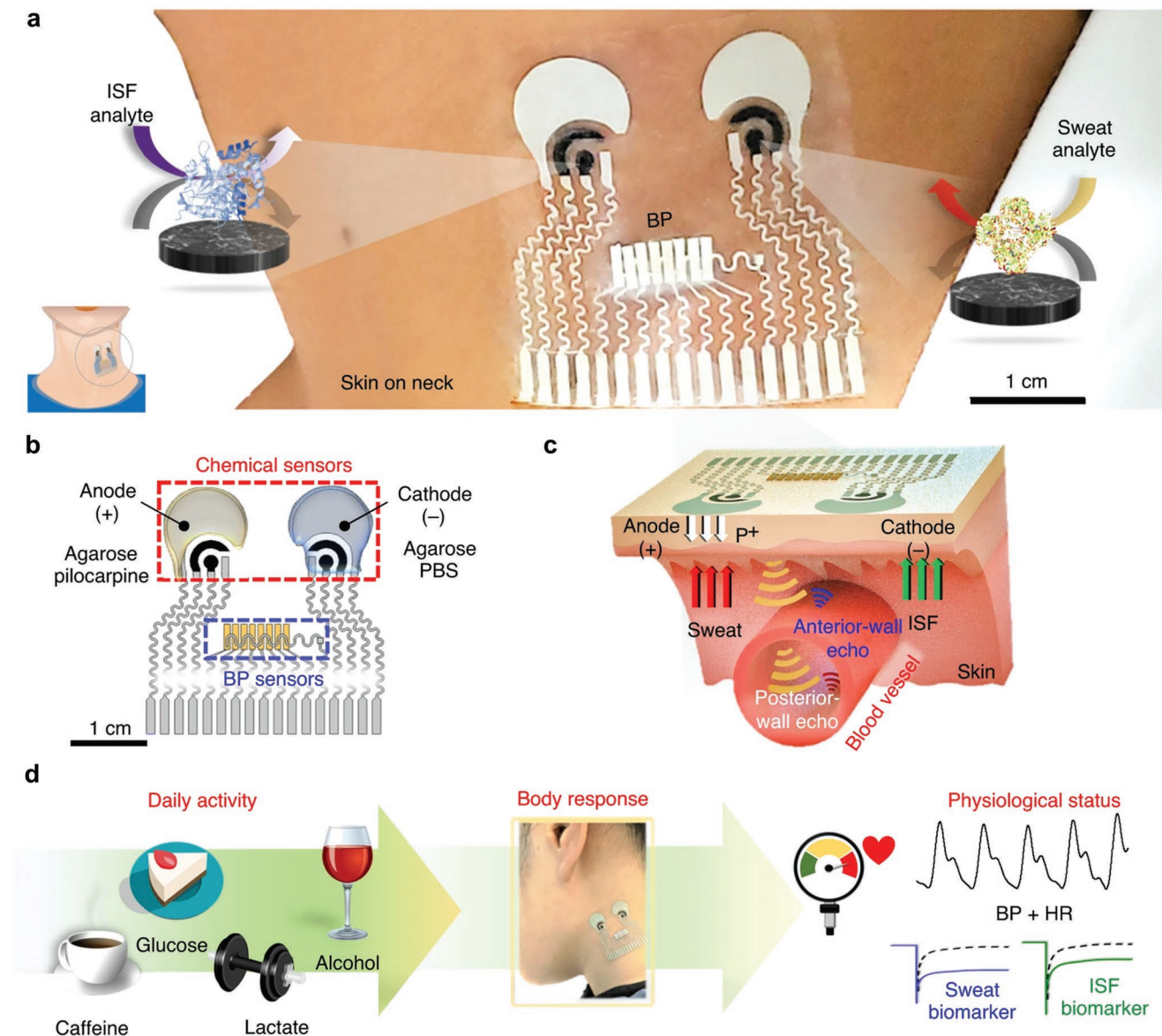


Figure 10. Recent representative studies on wearable hydrogel patches for biological sensing. a) Illustration for the attachment of the sensor on the skin. b) Illustration of the acoustic and electrochemical sensing components of the sensor along with hydrogels. c) Acoustic sensing and iontophoresis mechanism of the integrated sensor. d) An integrated wearable soft agarose gel sensor with high mechanical resiliency and high selectivity for glucose, lactate, caffeine, alcohol, blood pressure, and heart rate probing. Reproduced with permission.^[90c] Copyright 2021, Springer Nature.

any discomfort and skin damage during removal. From the commercialization perspective, researchers should keep in mind not to use complicated and multi-step fabrication processes, which follow the high cost of multifunctional skin adhesive patch development. Limited reusability, smart reversibility in adhesion, and difficulty in handling are certain critical concerns that must be overcome. Therefore, a simple and cost-effective way still needs to be developed for the practical use of robust, bioinspired, skin-friendly, and biocompatible skin adhesive patches. For instance, the experimental approach for fabricating hydrogel patches can be confined to directly mixing several experimental parameters, including i) total polymer content, ii) type of cations, iii) concentration of gelation ions,

and iv) polymer ratio between various polymer chains.^[163] Ideally, one-pot synthesis of the hydrogel patch with these strictly controlled parameters is desirable for robust production on an industrial scale with low cost. Furthermore, researchers should pay more attention to the adhesion mechanism than cohesion. Cohesion intensely affects how the adhesives will be used, which is particularly important for clinical translation.

Furthermore, we have highlighted the most prominent approaches and latest progress involving representative examples of modern wearable patches for biomedical applications, including wound healing and drug delivery, energy harvesting, physiochemical biosensing, and motion and health monitoring. These findings have illustrated the biocompatibility and

Table 5. Summary of recent hydrogel patches for various biomedical applications.

Type	Materials	Elastic modulus	Adhesion energy or conductivity	Applications	Ref.
Transdermal patch	Polyacrylamide, polydopamine and mesoporous silica NPs	≈70 kPa	15.3 J m ⁻²	Adhesive transdermal patch for efficient controlled drug delivery	[22]
pH-actuated skin patch	Poly mAA-co-AAm (methacrylic acids and acrylamide) and PDMS	8 kPa (Maximum back pressure)	N/A	Sensitive to low pH of chronic/infected wounds to deliver antibiotics	[84]
Diabetic wound patch	Polyurethane, chitosan and poly(acrylic acid) grafted with N-hydroxysuccinimide ester	≈40 kPa for hydrated state; ≈5 GPa for glassy state	650 J m ⁻²	Stain-programmed patch for physically guiding diabetic wound closure	[85]
E-skin for sweat sensing	Polyvinyl alcohol and agarose-glycerol	70 kPa	N/A	Rapid detection of thermoregulatory sweat rate at nL min ⁻¹ cm ⁻² with the sweat composition at rest	[90f]
E-tattoo for bio-electrodes	Silk fibroin, graphene and Ca ²⁺ integrated	N/A	1.61 to 3.57 (Ω m) ⁻¹ from 20 to 50 °C	High sensitivity, fast response and long-term stability for detection of ECG, breathing, and temperature, strain, humidity, and temperature	[103]
Motion sensing patch	Acrylamide and N-hydroxy methyl acrylamide with βcyclodextrin	88 kPa	Adhesive strength: ≈34.5 ± 1.7 kPa for skin	Rapid detection of both robust (index finger and wrist) and tiny (swallowing and phonation) motions	[39]
A hydrogel patch-based triboelectric nanogenerator	Polyacrylic acid (PAA), elastomer (Ecoflex 00–30) and Cu-doped ZnS NPs	51 kPa; can be subject to a high strain of 700%	N/A	Demonstrating touch-sensing with efficient energy harvesting for high voltage and power density output; high sensitivity of pressure; and light-emitting response as a smart skin	[129]

N/A denotes “not available.”

superior functionalities of hydrogel-based wearable devices with great promise for POC diagnosis and therapy. This progress is benefited from the refinement of multiplexed physiochemical sensing platforms, implementation of nanotechnology, and polymer chemistry for improved small-scale biosensing and local therapy to reduce side effects, costs, and difficulties compared to conventional methods. Stimuli-responsive self-powered/energy harvester-based skin patches would be the next-generation trend of successful wearable devices to meet the demand of multiple power consumption as a portable device and signal readout measurement: 1) analytes detection; 2) analyte signal processing; and 3) signal transmission (e.g., wireless communication) for physiological data collection or analyte-triggered drug delivery for therapy. Most biochemical wearable skin patches may not require batteries to launch their functionalities for convenience, thereby producing specific therapeutic outcomes without understanding the status of the disease in real-time. The recent advanced approaches, including energy harvesting and storage devices (e.g., piezoelectric, triboelectric, or a combination of sources) that utilize analytes as the fuel to empower biosensing, signal processing, data transmission, or/and potentially release the desired drugs for treatment, depending on the purpose. Together, wearable skin

patches would not only be a simple patch for simple sensing or controlled release but potentially be digitalized or self-powered for a miniature soft theragnostic device in the future.

We believe that significant advances have already set a good foundation for material development and electronics. However, more engineering is still required to assimilate a suitable design and protocol that can take the technology to the commercial market. In order to achieve utterly biocompatible skin patches, novel biomaterials with high mechanical properties need to be explored and sophisticated techniques need to be adopted to fabricate these patches to make them economical and viable. Besides, an in-depth understanding of each component is required to fabricate long-term biocompatible skin patches. Moreover, the utilization of natural polymers needs to be emphasized from an ecological point of view. Considering these aspects, future development should focus on easy procedures with environment-friendly and cost-effective materials that can be blended to manufacture a handy skin-patchable device with multipurpose features. The interdisciplinary collaborative efforts of engineers, biologists, medical doctors, and researchers will be needed to merge the knowledge and skills of different fields to achieve this milestone. Indeed, the healthcare industry may witness a major revolution in the coming years.

Acknowledgements

The work was supported within the framework of a European Regional Development Fund Project, under the title Application of Modern Technologies in Medicine and Industry (No. CZ.02.1.01/0.0/0.0/17_048/0007280). S.H.D.W. acknowledges the Start-up Funding (0033912) from the Department of Biomedical Engineering and Start-up Fund for RAPS under the Strategic Hiring Scheme (0035876), the Hong Kong Polytechnic University (PolyU, University Grant Council), and PolyU Projects of RISports (0043522) for supporting this work. J.Y. acknowledges the Basic Science Research Program (2022R1A2C2008256) supported by the Ministry of Science and ICT and the National Research Foundation of Korea.

Conflict of Interest

The authors declare no conflict of interest.

Keywords

biomedical applications, design strategy, E-skin patches, skin adhesive patches, transdermal patches, wearable patches

Received: November 21, 2022

Revised: December 23, 2022

Published online:

- [1] Z. Ma, S. Li, H. Wang, W. Cheng, Y. Li, L. Pan, Y. Shi, *J. Mater. Chem. B* **2019**, *7*, 173.
- [2] Y. Chen, Q. An, K. X. Teng, Y. H. Zhang, Y. T. Zhao, *Eur. Polym. J.* **2022**, *170*, 111164.
- [3] A. C. Bunea, V. Dediu, E. A. Laszlo, F. Pistritu, M. Carp, F. S. Ilescu, O. N. Ionescu, C. Ilescu, *Micromachines* **2021**, *12*, 1091.
- [4] H. Lee, C. Song, S. Baik, D. Kim, T. Hyeon, D. H. Kim, *Adv. Drug Delivery Rev.* **2018**, *127*, 35.
- [5] M. Bok, Z. J. Zhao, S. H. Hwang, Y. Jeong, J. Ko, J. Ahn, J. H. Lee, S. Jeon, J. H. Jeong, *ACS Appl. Mater. Interfaces* **2021**, *13*, 58220.
- [6] S. H. Jeong, Y. Lee, M. G. Lee, W. J. Song, J. U. Park, J. Y. Sun, *Nano Energy* **2021**, *79*, 105463.
- [7] T. L. Wu, C. Y. Cui, Y. T. Huang, Y. Liu, C. C. Fan, X. X. Han, Y. Yang, Z. Y. Xu, B. Liu, G. W. Fan, W. G. Liu, *ACS Appl. Mater. Interfaces* **2020**, *12*, 2039.
- [8] M. H. Tan, X. H. Xu, T. J. Yuan, X. Hou, J. Wang, Z. H. Jiang, L. H. Peng, *Biomaterials* **2022**, *283*, 121413.
- [9] Q. Bai, J. C. Zhang, Y. X. Yu, C. H. Zhang, Y. J. Jiang, D. Q. Yang, M. H. Liu, L. N. Wang, F. L. Du, N. Sui, Z. L. Zhu, *ACS Appl. Mater. Interfaces* **2022**, *14*, 26455.
- [10] a) J. Lee, B. S. Lee, S. Baik, D. Kim, N. J. Park, J. W. Lee, S. K. Bong, S. H. Lee, S. N. Kim, J. H. Song, J. K. Kim, G. R. Yi, K. H. Kim, C. Pang, *Chem. Eng. J.* **2022**, *444*, 136581; b) A. G. Tabriz, D. Douroumis, *J. Drug Delivery Sci. Technol.* **2022**, *74*, 103564.
- [11] J. C. Tsai, R. H. Guy, C. R. Thornfeldt, W. N. Gao, K. R. Feingold, P. M. Elias, *J. Pharm. Sci.* **1996**, *85*, 643.
- [12] B. Godin, E. Toutou, *Crit. Rev. Ther. Drug.* **2003**, *20*, 63.
- [13] a) J. Yang, X. Liu, Y. Fu, Y. Song, *Acta Pharm. Sin. B* **2019**, *9*, 469; b) H. C. Koydemir, A. Ozcan, *Annu. Rev. Anal. Chem.* **2018**, *11*, 127; c) N. S. Rejinold, J. H. Shin, H. Y. Seok, Y. C. Kim, *Expert Opin. Drug Delivery* **2016**, *13*, 109.
- [14] a) H. Jin, Y. S. Abu-Raya, H. Haick, *Adv. Healthcare Mater.* **2017**, *6*, 1700024; b) D. H. Kim, R. Ghaffari, N. S. Lu, S. D. Wang, S. P. Lee, H. Keum, R. D'Angelo, L. Klinker, Y. W. Su, C. F. Lu, Y. S. Kim, A. Ameen, Y. H. Li, Y. H. Zhang, B. de Graff, Y. Y. Hsu, Z. J. Liu, J. Ruskin, L. Z. Xu, C. Lu, F. G. Omenetto, Y. G. Huang, M. Mansour, M. J. Slepian, J. A. Rogers, *Proc. Natl. Acad. Sci. USA* **2012**, *109*, 19910; c) J. Kim, R. Ghaffari, D. H. Kim, *Nat. Biomed. Eng.* **2017**, *1*, 0049; d) H. Lee, C. Song, S. Baik, D. Kim, T. Hyeon, D. H. Kim, *Adv. Drug Delivery Rev.* **2018**, *127*, 35; e) M. R. Prausnitz, R. Langer, *Nat. Biotechnol.* **2008**, *26*, 1261; f) I. Hwang, H. N. Kim, M. Seong, S. H. Lee, M. Kang, H. Yi, W. G. Bae, M. K. Kwak, H. E. Jeong, *Adv. Healthcare Mater.* **2018**, *7*, 1800275.
- [15] a) H. Yuk, C. E. Varela, C. S. Nabzdyk, X. Y. Mao, R. F. Padera, E. T. Roche, X. H. Zhao, *Nature* **2019**, *575*, 169; b) C. Ghobril, M. W. Grinstaff, *Chem. Soc. Rev.* **2015**, *44*, 1820.
- [16] C. Maiti, K. B. C. Imani, J. Yoon, *ChemPlusChem* **2021**, *86*, 601.
- [17] M. S. Jhon, J. D. Andrade, *J. Biomed. Mater. Res.* **1973**, *7*, 509.
- [18] a) G. Bovone, O. Y. Dudaryeva, B. Marco-Dufort, M. W. Tibbitt, *ACS Biomater. Sci. Eng.* **2021**, *7*, 4048; b) W. W. Liu, C. Zhang, Y. P. Bai, *J. Adhes. Sci. Technol.* **2021**, *35*, 111.
- [19] a) C. H. Yang, Z. G. Suo, *Nat. Rev. Mater.* **2018**, *3*, 125; b) X. Y. Liu, J. Liu, S. T. Lin, X. H. Zhao, *Mater. Today* **2020**, *36*, 102.
- [20] a) P. K. Forooshani, B. P. Lee, *J. Polym. Sci. Polym. Chem.* **2017**, *55*, 9; b) B. P. Lee, P. B. Messersmith, J. N. Israelachvili, J. H. Waite, *Annu. Rev. Mater. Res.* **2011**, *41*, 99; c) W. Zhang, R. X. Wang, Z. M. Sun, X. W. Zhu, Q. Zhao, T. F. Zhang, A. Cholewinski, F. Yang, B. X. Zhao, R. Pinnaratip, P. K. Forooshani, B. P. Lee, *Chem. Soc. Rev.* **2020**, *49*, 433.
- [21] E. Khare, N. Holten-Andersen, M. J. Buehler, *Nat. Rev. Mater.* **2021**, *6*, 421.
- [22] H. Jung, M. K. Kim, J. Y. Lee, S. W. Choi, J. Kim, *Adv. Funct. Mater.* **2020**, *30*, 2004407.
- [23] L. Han, K. Z. Liu, M. H. Wang, K. F. Wang, L. M. Fang, H. T. Chen, J. Zhou, X. Lu, *Adv. Funct. Mater.* **2018**, *28*, 1704195.
- [24] G. G. Yang, K. H. Zhu, W. Guo, D. R. Wu, X. L. Quan, X. Huang, S. Y. Liu, Y. Y. Li, H. Fang, Y. Q. Qiu, Q. Y. Zheng, M. L. Zhu, J. Huang, Z. G. Zeng, Z. P. Yin, H. Wu, *Adv. Funct. Mater.* **2022**, *32*, 2200457.
- [25] Y. Liu, C. Wang, J. T. Xue, G. H. Huang, S. Zheng, K. Zhao, J. Huang, Y. Q. Wang, Y. Zhang, T. L. Yin, Z. Li, *Adv. Healthcare Mater.* **2022**, *11*, 2200653.
- [26] K. K. Kenneth Langstreth Johnson, A. D. Roberts, *Proc. R. Soc. London, Ser. A* **1971**, *324*, 301.
- [27] A. I. Vakis, V. A. Yastrebov, J. Scheibert, L. Nicola, D. Dini, C. Minfray, A. Almqvist, M. Paggi, S. Lee, G. Limbert, J. F. Molinari, G. Ancaux, R. Aghababaei, S. E. Restrepo, A. Papangelo, A. Cammarata, P. Nicolini, C. Putignano, G. Carbone, S. Stupkiewicz, J. Lengiewicz, G. Costagliola, F. Borgia, R. Guarino, N. M. Pugno, M. H. Muser, M. Ciavarella, *Tribol. Int.* **2018**, *125*, 169.
- [28] K. Kendall, *J. Phys. D: Appl. Phys.* **1975**, *8*, 1449.
- [29] a) F. Borgia, S. Colella, V. Mattoli, B. Mazzolai, N. M. Pugno, *RSC Adv.* **2014**, *4*, 25447; b) L. Brely, F. Borgia, N. M. Pugno, *Interface Focus* **2015**, *5*, 20140051; c) D. Misseroni, L. Afferrante, G. Carbone, N. M. Pugno, *J. Adhes.* **2018**, *94*, 46.
- [30] a) Y. J. Zhang, T. H. Tao, *Adv. Mater.* **2019**, *31*, 1905767; b) K. Zulkowski, *Adv. Skin Wound Care* **2017**, *30*, 372.
- [31] J. H. Lee, D. S. Lee, Y. C. Jung, J. W. Oh, Y. H. Na, *ACS Appl. Mater. Interfaces* **2021**, *13*, 8889.
- [32] Y. Jiang, X. Zhang, W. Zhang, M. Wang, L. Yan, K. Wang, L. Han, X. Lu, *ACS Nano* **2022**, *16*, 8662.
- [33] a) L. K. Borden, A. Gargava, S. R. Raghavan, *Nat. Commun.* **2021**, *12*, 4419; b) J. Deng, H. Yuk, J. J. Wu, C. E. Varela, X. Y. Chen, E. T. Roche, C. F. Guo, X. H. Zhao, *Nat. Mater.* **2021**, *20*, 229; c) Y. N. Jiang, X. Zhang, W. Zhang, M. H. Wang, L. W. Yan, K. F. Wang, L. Han, X. Lu, *ACS Nano* **2022**, *16*, 8662; d) X. F. Shi, P. Y. Wu, *Small* **2021**, *17*, 2101220.
- [34] Y. W. Jiang, A. A. Trotsyuk, S. M. Niu, D. Henn, K. Chen, C. C. Shih, M. R. Larson, A. M. Mermin-Bunnell, S. Mittal, J. C. Lai,

- A. Saberi, E. Beard, S. Jing, D. L. Zhong, S. R. Steele, K. F. Sun, T. Jain, E. Zhao, C. R. Neimeth, W. G. Viana, J. Tang, D. Sivaraj, J. Padmanabhan, M. Rodrigues, D. P. Perrault, A. Chattopadhyay, Z. N. Maan, M. C. Leolou, C. A. Bonham, S. H. Kwon, et al., *Nat. Biotechnol.* **2022**, 015283.
- [35] M. J. Tsai, I. J. Lu, Y. S. Fu, Y. P. Fang, Y. B. Huang, P. C. Wu, *Colloids Surf., B* **2016**, 148, 650.
- [36] B. Y. Kamal Saroha, B. Sharma, *Int. J. Curr. Pharm. Res.* **2011**, 3, 98.
- [37] O. A. Al Hanbali, H. M. S. Khan, M. Sarfraz, M. Arafat, S. Ijaz, A. Hameed, *Acta Pharmaceut.* **2019**, 69, 197.
- [38] Z. Wang, J. Wang, H. Li, J. Yu, G. Chen, A. R. Kahkoska, V. Wu, Y. Zeng, D. Wen, J. R. Miedema, J. B. Buse, Z. Gu, *Proc. Natl. Acad. Sci. USA* **2020**, 117, 29512.
- [39] A. Roy, K. Manna, P. G. Ray, S. Dhara, S. Pal, *ACS Appl. Mater. Interfaces* **2022**, 14, 17065.
- [40] M. Amjadi, D. Sheykhsari, B. J. Nelson, M. Sitti, *Adv. Mater.* **2018**, 30, 1704530.
- [41] M. B. Brown, G. P. Martin, S. A. Jones, F. K. Akomeah, *Drug Delivery* **2006**, 13, 175.
- [42] A. C. Williams, B. W. Barry, *Adv. Drug Delivery Rev.* **2004**, 56, 603.
- [43] S. Venkatraman, R. Gale, *Biomaterials* **1998**, 19, 1119.
- [44] a) R. H. Guy, Y. N. Kalia, M. B. Delgado-Charro, V. Merino, A. Lopez, D. Marro, *J. Controlled Release* **2000**, 64, 129; b) Y. N. Kalia, A. Naik, J. Garrison, R. H. Guy, *Adv. Drug Delivery Rev.* **2004**, 56, 619; c) A. K. Banga, S. Bose, T. K. Ghosh, *Int. J. Pharmaceut.* **1999**, 179, 10053197.
- [45] a) M. R. Prausnitz, *Adv. Drug Delivery Rev.* **2004**, 56, 581; b) A. R. Denet, R. Vanbever, V. Preat, *Adv. Drug Delivery Rev.* **2004**, 56, 659.
- [46] M. K. A. Arunachalam, D. Vinay Kumar, M. Prathap, S. Sethuraman, S. Ashutosh kumar, S. Manidipa, *Curr. Pharma Res.* **2010**, 1, 70.
- [47] a) M. P. D. Kapoor, M. Singhal, *Int. Pharm. Sci.* **2011**, 1, 54; b) S. Kamboj, V. Jhawar, V. Saini, S. Bala, *Curr. Drug Ther.* **2013**, 8, 181; c) A. Ahad, M. Aqil, K. Kohli, Y. Sultana, M. Mujeeb, *Artif Cells Nanomed. Biotechnol.* **2016**, 44, 1457.
- [48] A. C. Williams, B. W. Barry, *Adv. Drug Delivery Rev.* **2004**, 56, 603.
- [49] M. Isaac, C. Holvey, *Ther. Adv. Psychopharmacol.* **2012**, 2, 255.
- [50] T. G. S. Sunita Dhiman, A. K. Rehni, *Int. J. Pharm. Pharm. Sci.* **2011**, 3, 26.
- [51] S. Mutalik, N. Udupa, *Clin. Exp. Pharmacol. Physiol.* **2006**, 33, 17.
- [52] C. L. Stevenson, J. T. Santini, Jr., R. Langer, *Adv. Drug Delivery Rev.* **2012**, 64, 1590.
- [53] V. Phatale, K. K. Vaiphei, S. Jha, D. Patil, M. Agrawal, A. Alexander, *J. Controlled Release* **2022**, 351, 361.
- [54] P. R. P. Verma, S. S. Iyer, *J. Pharm. Pharmacol.* **2000**, 52, 151.
- [55] V. Carelli, S. Coltelli, G. Di Colo, E. Nannipieri, M. F. Serafini, *Int. J. Pharm.* **1999**, 179, 73.
- [56] H. Gabiga, K. Cal, S. Janicki, *Int. J. Pharm.* **2000**, 199, 10794921.
- [57] T. Loftsson, A. M. Siguroardottir, *Eur. J. Pharm. Sci.* **1994**, 2, 297.
- [58] J. Kim, Y. Cho, H. Choi, *Int. J. Pharm.* **2000**, 196, 105.
- [59] O. A. Al Hanbali, H. M. S. Khan, M. Sarfraz, M. Arafat, S. Ijaz, A. Hameed, *Acta Pharm.* **2019**, 69, 197.
- [60] D. M. Panchaxari, S. Pampana, T. Pal, B. Devabhaktuni, A. K. Aravapalli, *Daru* **2013**, 21, 6.
- [61] S. M. Al-Saidan, Y. S. R. Krishnaiah, D. V. Chandrasekhar, J. K. Lalla, B. Rama, B. Jayaram, P. Bhaskar, *Skin Pharmacol. Phys.* **2004**, 17, 310.
- [62] Y. S. Krishnaiah, P. Bhaskar, V. Satyanarayana, *Drug Delivery* **2004**, 11, 1.
- [63] a) A. Z. Alkilani, M. T. McCrudden, R. F. Donnelly, *Pharmaceutics* **2015**, 7, 438; b) H. Trommer, R. H. Neubert, *Skin Pharmacol. Physiol.* **2006**, 19, 106.
- [64] P. M. Satturwar, S. V. Fulzele, A. K. Dorle, *AAPS PharmSciTech* **2005**, 6, E649.
- [65] I. Zurdo Schroeder, P. Franke, U. F. Schaefer, C. M. Lehr, *J. Controlled Release* **2007**, 118, 196.
- [66] I. Som, K. Bhatia, M. Yasir, *J. Pharm. BioAllied Sci.* **2012**, 4, 2.
- [67] C. Yang, P. Quan, X. C. Liu, M. L. Wang, L. Fang, *Asian J. Pharm. Sci.* **2014**, 9, 51.
- [68] G. M. El Maghraby, A. C. Williams, B. W. Barry, *Int. J. Pharm.* **2004**, 276, 143.
- [69] a) R. Kumar, A. Philip, *Trop. J. Pharm. Res.* **2007**, 6, 633; b) R. K. Tyagi, A. Chandra, D. Singh, M. A. Rahman, *Int. J. Pharm. Sci. Res.* **2011**, 2, 1379.
- [70] S. Banerjee, P. Chattopadhyay, A. Ghosh, P. Datta, V. Veer, *Int. J. Adhes. Adhes.* **2014**, 50, 70.
- [71] A. K. Z. Czech, J. Swiderska, Wide spectra of quality control, **2011**, 17, 310.
- [72] Y. P. Su, W. X. Lu, X. L. Fu, Y. Xu, L. X. Ye, J. Yang, H. H. Huang, C. X. Yu, *AAPS PharmSciTech* **2020**, 21, 297.
- [73] D. G. Maillard-Salin, P. Becourt, G. Couarraze, *Int. J. Pharm.* **2000**, 199, 29.
- [74] A. Santoro, L. C. Rovati, R. Lanzini, I. Setnikar, *Prog. Drug Res.* **2000**, 50, 897.
- [75] T. Nakajima-Kambe, Y. Shigeno-Akutsu, N. Nomura, F. Onuma, T. Nakahara, *Appl. Microbiol. Biotechnol.* **1999**, 51, 134.
- [76] N. S. H. Shyamala Bhaskaran, *Indian J. Pharm. Sci.* **2000**, 6, 424.
- [77] B. K. Dey, L. K. Nath, B. Mohanti, B. B. Bhowmik, *Indian J. Pharm. Educ. Res.* **2007**, 41, 388.
- [78] B. Yin, J. Ni, C. E. Witherel, M. Yang, J. A. Burdick, C. Wen, S. H. D. Wong, *Theranostics* **2022**, 12, 207.
- [79] B. Liu, B. W. Lee, K. Nakanishi, A. Villasante, R. Williamson, J. Metz, J. Kim, M. Kanai, L. Bi, K. Brown, G. Di Paolo, S. Homma, P. A. Sims, V. K. Topkara, G. Vunjak-Novakovic, *Nat. Biomed. Eng.* **2018**, 2, 293.
- [80] A. Tamayol, M. Akbari, Y. Zilberman, M. Comotto, E. Lesha, L. Serex, S. Bagherifard, Y. Chen, G. Q. Fu, S. K. Ameri, W. T. Ruan, E. L. Miller, M. R. Dokmeci, S. Sonkusale, A. Khademhosseini, *Adv. Healthcare Mater.* **2016**, 5, 711.
- [81] A. Ahsan, W.-X. Tian, M. A. Farooq, D. H. Khan, *Int. J. Polym. Mater. Polym. Biomater.* **2021**, 70, 574.
- [82] S. Guo, L. A. DiPietro, *J. Dent. Res.* **2010**, 89, 219.
- [83] a) J. Zhang, S. H. D. Wong, X. Wu, H. Lei, M. Qin, P. Shi, W. Wang, L. Bian, Y. Cao, *Adv. Mater.* **2021**, 33, 2105765; b) B. Yin, W. K. H. Ho, Q. Zhang, C. Li, Y. Huang, J. Yan, H. Yang, J. Hao, S. H. D. Wong, M. Yang, *ACS Appl. Mater. Interfaces* **2022**, 14, 4714; c) B. H. Yin, Q. Zhang, X. Y. Xia, C. Q. Li, W. K. H. Ho, J. X. Yan, Y. Y. Huang, H. L. Wu, P. Wang, C. Q. Yi, J. H. Hao, J. F. Wang, H. L. Chen, S. H. D. Wong, M. Yang, *Theranostics* **2022**, 12, 5914; d) S. H. D. Wong, X. Xu, X. Chen, Y. Xin, L. Xu, C. H. N. Lai, J. Oh, W. K. R. Wong, X. Wang, S. Han, W. You, X. Shuai, N. Wong, Y. Tan, L. Duan, L. Bian, *Nano Lett.* **2021**, 21, 3225.
- [84] H. Jiang, M. Ochoa, J. F. Waimin, R. Rahimi, B. Ziaie, *Lab Chip* **2019**, 19, 2265.
- [85] G. Theocharidis, H. Yuk, H. Roh, L. Wang, I. Mezghani, J. Wu, A. Kafanas, M. Contreras, B. Sumpio, Z. Li, E. Wang, L. Chen, C. F. Guo, N. Jayaswal, X. L. Katopodi, N. Kalavros, C. S. Nabzdyk, I. S. Vlachos, A. Veves, X. Zhao, *Nat. Biomed. Eng.* **2022**, 6, 118.
- [86] J. C. Gayet, G. Fortier, *J. Controlled Release* **1996**, 38, 177.
- [87] C. C. Chen, C. L. Fang, S. A. Al-Suwayeh, Y. L. Leu, J. Y. Fang, *Int. J. Pharm.* **2011**, 415, 119.
- [88] E. Beyssac, C. Bregni, J. M. Aiache, S. Gerula, E. Smolko, *Drug Dev. Ind. Pharm.* **1996**, 22, 439.
- [89] P. Kuzma, A. J. MooYoung, D. Moro, H. Quandt, C. W. Bardin, P. H. Schlegel, *Macromol. Symp.* **1996**, 109, 15.
- [90] a) H. Y. Y. Nyein, L.-C. Tai, Q. P. Ngo, M. Chao, G. B. Zhang, W. Gao, M. Bariya, J. Bullock, H. Kim, H. M. Fahad, A. Javey, *ACS Sens.* **2018**, 3, 944; b) T. Saha, J. Fang, S. Mukherjee, M. D. Dickey, O. D. Velev, *ACS Appl. Mater. Interfaces* **2021**, 13,

- 8071; c) J. R. Sempionatto, M. Lin, L. Yin, E. De La Paz, K. Pei, T. Sonsa-Ard, A. N. De Loyola Silva, A. A. Khorshed, F. Zhang, N. Tostado, S. Xu, J. Wang, *Nat. Biomed. Eng.* **2021**, 5, 737; d) L. Wang, T. Xu, X. He, X. Zhang, *J. Mater. Chem. C* **2021**, 9, 14938; e) F. J. Zhao, M. Bonmarin, Z. C. Chen, M. Larson, D. Fay, D. Runnoe, J. Heikenfeld, *Lab Chip* **2020**, 20, 168; f) H. Y. Y. Nyein, M. Bariya, B. Tran, C. H. Ahn, B. J. Brown, W. B. Ji, N. Davis, A. Javey, *Nat. Commun.* **2021**, 12, 1823.
- [91] S. Y. Xu, T. Y. Li, H. X. Ren, X. Y. Mao, X. S. Ye, B. Liang, in *2020 IEEE SENSORS*, **2020**.
- [92] A. Ahsan, M. A. Farooq, *J. Drug Delivery Sci. Technol.* **2019**, 54, 101308.
- [93] D. Wan, J. Yang, X. J. Cui, N. C. Ma, Z. S. Wang, Y. P. Li, P. W. Li, Y. X. Zhang, Z. H. Lin, S. B. Sang, H. L. Zhang, *Nano Energy* **2021**, 89, 106465.
- [94] C. Y. K. Lam, Q. Zhang, B. H. Yin, Y. Y. Huang, H. Wang, M. Yang, S. H. D. Wong, *J. Compos. Sci.* **2021**, 5, 190.
- [95] J. Kim, A. S. Campbell, B. E.-F. De Ávila, J. Wang, *Nat. Biotechnol.* **2019**, 37, 389.
- [96] S. Bashir, M. Hina, J. Iqbal, A. H. Rajpar, M. A. Mujtaba, N. A. Alghamdi, S. Wageh, K. Ramesh, S. Ramesh, *Polymers* **2020**, 12, 2702.
- [97] S. Y. Zhang, S. B. Li, Z. Z. L. Xia, K. Y. Cai, *J. Mater. Chem. B* **2020**, 8, 852.
- [98] B. Ying, X. Liu, *iScience* **2021**, 24, 103174.
- [99] L. B. Baker, *Temperature* **2019**, 6, 211.
- [100] K. Sato, *Rev. Physiol. Biochem. Pharmacol.* **1977**, 79, 51.
- [101] a) I. Alvear-Ordenes, D. Garcia-Lopez, J. A. De Paz, J. Gonzalez-Gallego, *Int. J. Sports Med.* **2005**, 26, 632; b) T. T. Amatruda, L. G. Welt, *J. Appl. Physiol.* **1953**, 5, 759; c) L. B. Baker, C. T. Ungaro, B. C. Sopena, R. P. Nuccio, A. J. Reimel, J. M. Carter, J. R. Stofan, K. A. Barnes, *J. Appl. Physiol.* **2018**, 124, 1304.
- [102] P. F. Yang, G. F. Wei, A. Liu, F. W. Huo, Z. N. Zhang, *npj Flexible Electron.* **2022**, 6, 33.
- [103] Q. Wang, S. J. Ling, X. P. Liang, H. M. Wang, H. J. Lu, Y. Y. Zhang, *Adv. Funct. Mater.* **2019**, 29, 1808695.
- [104] H. Lee, Y. J. Hong, S. Baik, T. Hyeon, D. H. Kim, *Adv. Healthcare Mater.* **2018**, 7, 1701150.
- [105] Y. J. Lin, M. Bariya, H. Y. Y. Nyein, L. Kivimaki, S. Uusitalo, E. Jonsson, W. B. Ji, Z. Yuan, T. Happonen, C. Liedert, J. Hiltunen, Z. Y. Fan, A. Javey, *Adv. Funct. Mater.* **2019**, 29, 1902521.
- [106] Y. R. Yang, Y. Song, X. J. Bo, J. H. Min, O. S. Pak, L. L. Zhu, M. Q. Wang, J. B. Tu, A. Kogan, H. X. Zhang, T. K. Hsiai, Z. P. Li, W. Gao, *Nat. Biotechnol.* **2020**, 38, 217.
- [107] a) V. Bhole, J. W. J. Choi, S. W. Kim, M. de Vera, H. Choi, *Am. J. Med.* **2010**, 123, 957; b) D. I. Feig, D. H. Kang, R. J. Johnson, *N. Engl. J. Med.* **2008**, 359, 1811; c) P. A. Russo, G. A. Mitchell, R. M. Tanguay, *Pediatr. Dev. Pathol.* **2001**, 4, 212; d) R. Terkeltaub, *Nat. Rev. Rheumatol.* **2010**, 6, 30.
- [108] Z. Cui, F. R. Pobleto, Y. Zhu, *ACS Appl. Mater. Interfaces* **2019**, 11, 17836.
- [109] J. C. Luo, S. J. Gao, H. Luo, L. Wang, X. W. Huang, Z. Guo, X. J. Lai, L. W. Lin, R. K. Y. Li, J. F. Gao, *Chem. Eng. J.* **2021**, 406, 126898.
- [110] T. Yokota, Y. Inoue, Y. Terakawa, J. Reeder, M. Kaltenbrunner, T. Ware, K. J. Yang, K. Mabuchi, T. Murakawa, M. Sekino, W. Voit, T. Sekitani, T. Someya, *Proc. Natl. Acad. Sci. USA* **2015**, 112, 14533.
- [111] M. Jung, K. Kim, B. Kim, H. Cheong, K. Shin, O. S. Kwon, J. J. Park, S. Jeon, *ACS Appl. Mater. Interfaces* **2017**, 9, 26974.
- [112] J. H. Oh, S. Y. Hong, H. Park, S. W. Jin, Y. R. Jeong, S. Y. Oh, J. Yun, H. Lee, J. W. Kim, J. S. Ha, *ACS Appl. Mater. Interfaces* **2018**, 10, 7263.
- [113] M. A. Rahman, S. Walia, S. Naznee, M. Taha, S. Nirantar, F. Rahman, M. Bhaskaran, S. Sriram, *Adv. Intell. Syst.* **2020**, 2, 2000094.
- [114] J. Feito, O. Garcia-Suarez, J. Garcia-Piqueras, Y. Garcia-Mesa, A. Perez-Sanchez, I. Suazo, R. Cabo, J. Suarez-Quintanilla, J. Cobo, J. A. Vega, *Ann. Anat.* **2018**, 219, 8.
- [115] M. L. Mcdermott, J. W. Chandler, *Surv. Ophthalmol.* **1989**, 33, 381.
- [116] J. Park, J. Kim, S. Y. Kim, W. H. Cheong, J. Jang, Y. G. Park, K. Na, Y. T. Kim, J. H. Heo, C. Y. Lee, J. H. Lee, F. Bien, J. U. Park, *Sci. Adv.* **2018**, 4, eaap9841.
- [117] N. M. Farandos, A. K. Yetisen, M. J. Monteiro, C. R. Lowe, S. H. Yun, *Adv. Healthcare Mater.* **2015**, 4, 792.
- [118] a) J. T. Baca, D. N. Finegold, S. A. Asher, *Ocul. Surf.* **2007**, 5, 280; b) L. Zhou, R. W. Beuerman, *Prog. Retinal Eye Res.* **2012**, 31, 527.
- [119] M. X. Chu, K. Miyajima, D. Takahashi, T. Arakawa, K. Sano, S. Sawada, H. Kudo, Y. Iwasaki, K. Akiyoshi, M. Mochizuki, K. Mitsubayashi, *Talanta* **2011**, 83, 960.
- [120] M. Leonardi, E. M. Pitchon, A. Bertsch, P. Renaud, A. Mermoud, *Acta Ophthalmol.* **2009**, 87, 433.
- [121] W. J. Liu, Z. H. Long, G. Y. Yang, L. L. Xing, *Biosensors* **2022**, 12, 60.
- [122] J.-N. Kim, J. Lee, H. Lee, I.-K. Oh, *Nano Energy* **2021**, 82, 105705.
- [123] T. Cheng, Y. Z. Zhang, S. Wang, Y. L. Chen, S. Y. Gao, F. Wang, W. Y. Lai, W. Huang, *Adv. Funct. Mater.* **2021**, 31, 2101303.
- [124] C. Wu, P. Jiang, W. Li, H. Guo, J. Wang, J. Chen, M. R. Prausnitz, Z. L. Wang, *Adv. Funct. Mater.* **2020**, 30, 1907378.
- [125] W. Zhang, P. Feng, J. Chen, Z. Sun, B. Zhao, *Prog. Polym. Sci.* **2019**, 88, 220.
- [126] T. G. Yun, M. Park, D.-H. Kim, D. Kim, J. Y. Cheong, J. G. Bae, S. M. Han, I.-D. Kim, *ACS Nano* **2019**, 13, 3141.
- [127] Z. H. Jin, F. Z. Zhao, Y. L. Lei, Y. C. Wang, *Nano Energy* **2022**, 95, 106988.
- [128] S. Liu, Y. Zhong, X. Zhang, M. Pi, X. Wang, R. Zhu, W. Cui, R. Ran, *ACS Appl. Mater. Interfaces* **2022**, 14, 15641.
- [129] G. Liang, Z. Ruan, Z. Liu, H. Li, Z. Wang, Z. Tang, F. Mo, Q. Yang, L. Ma, D. Wang, C. Zhi, *Adv. Electron. Mater.* **2019**, 5, 1900553.
- [130] W. Xu, L. B. Huang, M. C. Wong, L. Chen, G. Bai, J. Hao, *Adv. Energy Mater.* **2017**, 7, 1601529.
- [131] X. Jing, H. Li, H.-Y. Mi, P.-Y. Feng, X. Tao, Y. Liu, C. Liu, C. Shen, *J. Mater. Chem. C* **2020**, 8, 5752.
- [132] S. J. Zheng, W. Z. Li, Y. Y. Ren, Z. Y. Liu, X. Y. Zou, Y. Hu, J. N. Guo, Z. Sun, F. Yan, *Adv. Mater.* **2022**, 34, 2106570.
- [133] R. Matsukawa, A. Miyamoto, T. Yokota, T. Someya, *Adv. Healthcare Mater.* **2020**, 9, 2001322.
- [134] Y. Yang, T. R. Cui, D. Li, S. R. Ji, Z. K. Chen, W. C. Shao, H. F. Liu, T. L. Ren, *Nano-Micro Lett.* **2022**, 14, 161.
- [135] Y. J. Hong, H. Jeong, K. W. Cho, N. Lu, D. H. Kim, *Adv. Funct. Mater.* **2019**, 29, 1808247.
- [136] L. Eskandarian, A. Toossi, F. Nassif, S. G. Rostami, S. T. Ni, A. Mahnam, M. A. Meghraz, W. Takarada, T. Kikutani, H. E. Naguib, *Adv. Mater.* **2022**, 7, 2101572.
- [137] Y. C. Qiao, X. S. Li, J. M. Jian, Q. Wu, Y. H. Wei, H. Shuai, T. Hirtz, Y. Zhi, G. Deng, Y. F. Wang, G. Y. Gou, J. D. Xu, T. R. Cui, H. Tian, Y. Yang, T. L. Ren, *ACS Appl. Mater. Interfaces* **2020**, 12, 49945.
- [138] R. T. Li, S. R. Kling, M. J. Salata, S. A. Cupp, J. Sheehan, J. E. Voos, *Sports Health* **2016**, 8, 74.
- [139] P. Kakria, N. K. Tripathi, P. Kitipawang, *Int. J. Telemed. Appl.* **2015**, 2015, 373474.
- [140] N. Kim, T. Lim, K. Song, S. Yang, J. Lee, *ACS Appl. Mater. Interfaces* **2016**, 8, 21070.
- [141] Y. H. Liu, J. J. S. Norton, R. Qazi, Z. N. Zou, K. R. Ammann, H. Liu, L. Q. Yan, P. L. Tran, K. I. Jang, J. W. Lee, D. Zhang, K. A. Kilian, S. H. Jung, T. Bretl, J. L. Xiao, M. J. Slepian, Y. G. Huang, J. W. Jeong, J. A. Rogers, *Sci. Adv.* **2016**, 2, 1601185.
- [142] X. Q. Yang, S. Q. Wang, M. Y. Liu, L. H. Li, Y. Y. Zhao, Y. F. Wang, Y. Y. Bai, Q. F. Lu, Z. P. Xiong, S. M. Feng, T. Zhang, *Small* **2022**, 18.
- [143] B. X. Xu, A. Akhtar, Y. H. Liu, H. Chen, W. H. Yeo, S. I. I. Park, B. Boyce, H. Kim, J. W. Yu, H. Y. Lai, S. Y. Jung, Y. H. Zhou, J. Kim, S. Cho, Y. G. Huang, T. Bretl, J. A. Rogers, *Adv. Mater.* **2016**, 28, 4462.

- [144] C. Wang, T. Yokota, T. Someya, *Chem. Rev.* **2021**, 121, 2109.
- [145] P. A. Lopes, D. Vaz Gomes, D. Green Marques, P. Faia, J. Gois, T. F. Patricio, J. Coelho, A. Serra, A. T. de Almeida, C. Majidi, M. Tavakoli, *Adv. Healthcare Mater.* **2019**, 8, 1900234.
- [146] G.-H. Lee, H. Moon, H. Kim, G. H. Lee, W. Kwon, S. Yoo, D. Myung, S. H. Yun, Z. Bao, S. K. Hahn, *Nat. Rev. Mater.* **2020**, 5, 149.
- [147] Y. Nam, B. Koo, A. Cichocki, S. Choi, *IEEE Trans. Bio-Med Eng.* **2014**, 61, 453.
- [148] R. Rac-Lubashevsky, H. A. Slagter, Y. Kessler, *Stem Cells Int.* **2017**, 7, 2547.
- [149] S. K. Ameri, M. Kim, I. A. Kuang, W. K. Perera, M. Alshiekh, H. Jeong, U. Topcu, D. Akinwande, N. S. Lu, *npj 2D Mater. Appl.* **2018**, 2, 19.
- [150] T. H. Hsieh, M. H. Liu, C. E. Kuo, Y. H. Wang, S. F. Liang, *J. Med. Biol. Eng.* **2021**, 41, 659.
- [151] W. T. Dong, L. Yang, R. Gravina, G. Fortino, *Inf. Fusion* **2021**, 71, 99.
- [152] S. Wan, N. Wu, Y. Ye, S. Li, H. Huang, L. Chen, H. Bi, L. Sun, *Small Struct.* **2021**, 2, 2100105.
- [153] Y. C. Qiao, X. S. Li, J. B. Wang, S. R. Ji, T. Hirtz, H. Tian, J. M. Jian, T. R. Cui, Y. Dong, X. W. Xu, F. Wang, H. Wang, J. H. Zhou, Y. Yang, T. Someya, T. L. Ren, *Small* **2022**, 18, 2104810.
- [154] C. Wang, H. Wang, B. Wang, H. Miyata, Y. Wang, M. O. G. Nayeem, J. J. Kim, S. Lee, T. Yokota, H. Onodera, T. Someya, *Sci. Adv.* **2022**, 8, eabo1396.
- [155] M. van Dooren, J. J. G. de Vries, J. H. Janssen, *Physiol. Behav.* **2012**, 106, 298.
- [156] A. Dzedzickis, A. Kaklauskas, V. Bucinskas, *Sensors* **2020**, 20, 592.
- [157] P. J. Lang, M. K. Greenwald, M. M. Bradley, A. O. Hamm, *Psychophysiology* **1993**, 30, 261.
- [158] a) G. Li, K. X. Huang, J. Deng, M. X. Guo, M. K. Cai, Y. Zhang, C. F. Guo, *Adv. Mater.* **2022**, 34, 2200261; b) H. Wu, G. G. Yang, K. H. Zhu, S. Y. Liu, W. Guo, Z. Jiang, Z. Li, *Adv. Sci.* **2021**, 8, 2001938.
- [159] a) H. U. Chung, A. Y. Rwei, A. Hourlier-Fargette, S. Xu, K. Y. Lee, E. C. Dunne, Z. Q. Xie, C. R. Liu, A. Carlini, D. H. Kim, D. Ryu, E. Kulikova, J. Y. Cao, I. C. Odland, K. B. Fields, B. Hopkins, A. Banks, C. Ogle, D. Grande, J. B. Park, J. Kim, M. Irie, H. Jang, J. H. Lee, Y. Park, J. Kim, H. H. Jo, H. Hahm, R. Avila, Y. H. Xu, et al., *Nat. Med.* **2020**, 26, 418; b) J. Heikenfeld, A. Jajack, J. Rogers, P. Gutruf, L. Tian, T. Pan, R. Li, M. Khine, J. Kim, J. Wang, J. Kim, *Lab Chip* **2018**, 18, 217; c) Y. J. Lin, M. Bariya, A. Javey, *Adv. Funct. Mater.* **2021**, 31, 2008087.
- [160] H. Jeong, J. A. Rogers, S. Xu, *Sci. Adv.* **2020**, 6, eabd4794.
- [161] E. Ghafar-Zadeh, *Sensors* **2015**, 15, 3236.
- [162] H. Y. Y. Nyein, L. C. Tai, Q. P. Ngo, M. H. Chao, G. B. Zhang, W. Gao, M. Bariya, J. Bullock, H. Kim, H. M. Fahad, A. Javey, *ACS Sens.* **2018**, 3, 944.
- [163] S. Mazzitelli, C. Pagano, D. Giusepponi, C. Nastruzzi, L. Perioli, *Int. J. Pharm.* **2013**, 454, 47.



Siu Hong Dexter Wong received his B.Eng. and Ph.D. degrees in Biomedical Engineering from the Chinese University of Hong Kong and was a visiting scholar at the Department of Chemistry at Stanford University. He is currently a research assistant professor of Department of Biomedical Engineering at the Hong Kong Polytechnic University. His research interests focus on the fabrication of novel nanomaterial and nano-composite hydrogel to investigate the nano-bio interface and harness ligand-receptor interaction for cellular mechanotransduction, tissue engineering, and immunotherapy. Moreover, he is also interested in exploring novel nanoplatforms for detection of viruses or biomarkers.



G. Roshan Deen attended Nanyang Technological University, Singapore and obtained his Ph.D. in Materials/Polymer Science. He has worked in the research groups of eminent scientists, Manfred Schmidt (University of Mainz), Masanori Hara (Rutgers University), and Jan Skov Pedersen (Aarhus University). He currently works at the Royal College of Surgeons in Ireland (RCSI), Medical University of Bahrain, and leads the Materials for Medicine Research Group. He is the co-PI of the Tissue Engineering Research Group of Middle East (TERG-ME), and the Diabetes Research Group. His research interests are in stimuli-responsive polymeric materials, and nanomaterials for versatile applications.



Jeffrey Bates is a faculty member in Materials Science and Engineering at the University of Utah. He received his doctoral degree in Materials Science and Engineering, where his research was on the development of stimuli-responsive hydrogels used as chemomechanical sensors that had the ability to monitor ion and pH conditions in biological media. His current work focuses on hydrogel materials used in drug delivery, sensing, and soft robotic applications, in addition to some exploratory work in sustainable polymer materials.



Jinhwan Yoon obtained his Ph.D. degree from Pohang University of Science and Technology (POSTECH), Korea. He worked as a postdoctoral researcher at POSTECH and the University of Massachusetts, Amherst. He is currently an associate professor at Pusan National University and is studying the design of mechanically reinforced novel crosslinked networks as well as the development of hybrid hydrogels and ionogels for highly stretchable soft matter devices.



Jagan Mohan Dodda obtained his Ph.D. in Chemistry from the Central Salt and Marine Chemicals Research Institute, Bhavnagar University, India. Later, he carried out his postdoctoral research at Akita University (Japan), Korea Forest Research Institute (South Korea), and the University Sains Malaysia (Malaysia). He is currently a senior researcher at the New Technology Research Centre, University of West Bohemia, Czech Republic. His current research focuses on multicomponent hydrogels based on the fundamental understanding of the structure–property relationships, for targeted biomedical applications.